The Constitutive Relation Error method: a general verification tool

Pierre Ladevèze, Ludovic Chamoin

The Constitutive Relation Error Method: A General Verification Tool

Pierre Ladevèze and Ludovic Chamoin

Abstract This chapter reviews the Constitutive Relation Error method as a general verification tool which is very suitable to compute strict and effective error bounds for linear and more generally convex Structural Mechanics problems. The review is focused on the basic features of the method and the most recent developments.

Keywords A posteriori error estimation · Constitutive relation error · Duality · Goal-oriented control · Nonlinear problems · PGD models

1 Introduction

Today, more than ever, modeling and simulation are central to any mechanical engineering activity. A constant concern both in industry and in research has always been the verification of models which nowadays can attain very high levels of complexity. The novelty of the situation is that over the last thirty years truly quantitative tools for assessing the quality of a FE model have appeared; this topic is now known as *model verification*. Of course, the original continuum mechanics model remains the reference. The state of the art can be found in [1–5]. Until the late 90s, only global error estimators were available through three different families introduced by [6–8]. Besides error indicators, adaptive computational approaches related to the mesh, time and iteration parameters have been developed for nearly all problems in Structural Mechanics. The CRE-verification method could be seen as a unified method in this context.

Since 1990, a key issue has become the evaluation of the quality of outputs of interest resulting from a finite element analysis. This objective was beyond the reach

P. Ladevèze (✉) · L. Chamoin
LMT (ENS Cachan, CNRS, Paris-Saclay University),
61 Avenue du Président Wilson, 94230 Cachan, France
e-mail: ladeveze@lmt.ens-cachan.fr

L. Chamoin
e-mail: chamoin@lmt.ens-cachan.fr

of earlier error estimators, which provided only global information which was totally insufficient for mechanical design purposes (design criteria involve local values of stresses, displacements, stress intensity factors,…). Among the numerous works on the linear case, we can mention [9–13] as the earliest ones; further references can be found in [2–5]. The main idea which emerged then was that an output of interest can be written globally, thus allowing the reuse of global error estimators; however, accurate error estimation requires the finite element solution of what is called the *adjoint problem*. Extensions to nonlinear time-dependent cases appeared in the late 90s [12, 14, 15]; these approaches consisted in getting back to the linear case through linearization during each time step.

Unfortunately, most of these estimates are not guaranteed to be upper or lower bounds, which is a very serious drawback for robust design. Consequently, one of today's research challenges is to derive upper error bounds for the calculated values of outputs of interest. Even in the linear case, relatively few works have proposed answers [1, 4, 9–11, 13, 16, 17]. Outside of the FE context, and only for the linear case, there are a few early works on this subject, such as [18, 19]. These, which use analytical Green functions, have serious limitations and seem quite remote from the present concern, in which numerical aspects are central.

Recent papers [20–22] introduced new upper error bounds on a computed output of interest for linear as well as time-dependent nonlinear problems, even in dynamics. These were probably the first strict upper bounds published for nonlinear and transient dynamics cases. Small-displacement problems without softening, such as (visco-)plasticity, were included through the standard thermodynamics framework involving internal state variables. Classical convexity properties were assumed. These works completed the a posteriori error estimation method developed particularly at LMT-Cachan, which was based on the concept of Constitutive Relation Error (CRE) of the dissipation type and on quasi-explicit techniques for the construction of associated admissible FE solutions.

The first key point of this approach was the integration of an output of interest in terms of finite variations; this led to the introduction of what is called the *mirror problem at time T*, which is very similar to the initial problem, as a substitute for the adjoint problem. Of course, the mirror problem coincides with the adjoint problem in the linear case. Another key point concerned the convexity properties, which constitute the true "engine" of our approach for deriving upper error bounds. These properties led to the basic relations between the dissipation-type constitutive relation error and the solution error. Eventually, upper error bounds were derived on the basis of the data and the FE solutions of both reference and mirror problems over the time-space domain being studied. It is also important to note that these bounds take all sources of error into account: time and space discretizations, ending of the iterations, and also modeling errors.

The present chapter goes in two directions. First, we give the main features of the CRE-method, going into details only for the linear case. Second, we introduce the advances performed recently. They mainly concern key technical points [23–27] and also various engineering problems [21, 22, 28–33]. Complex material models even in dynamics are considered and Constitutive Relation Errors are developed in [4].

The idea is rather simple; all equations are satisfied by admissible fields except the Constitutive Relation, so that the value of the residue related to the verification of the constitutive relation is an error indicator of the quality of the approximate solution. In other words, the approximate solution could be seen as the exact solution of the problem with a modified constitutive relation; then we compare this modified constitutive relation with the reference one. Here, we focus on upper error bounds and therefore only a particular class of material models is investigated, class characterized by convexity properties.

2 Reference Problem and Notations

Initially, the structure being studied occupies a domain $\Omega \subset \mathbb{R}^d$ with boundary $\partial\Omega$ (Fig. 1). We assume small displacements, quasi-static loading and isothermal conditions. The time interval of interest is denoted $[0, T]$. At any time t belonging to $[0, T]$, the structure is placed in an environment characterized by a displacement $\mathbf{U}_d$ on a part $\partial_1\Omega \subset \partial\Omega$, traction forces $\mathbf{F}_d$ on $\partial_2\Omega$ (the part of $\partial\Omega$ complementary to $\partial_1\Omega$), and body forces $\mathbf{f}_d$ within the domain Ω.

The problem which describes the evolution of the structure over $[0, T]$ is:

Find the displacement field $\mathbf{u}(\mathbf{x}, t)$ and the stress field $\sigma(\mathbf{x}, t)$, with $t \in [0, T]$ and $\mathbf{x} \in \Omega$, which verify:

- the kinematic constraints:

$$\mathbf{u} \in \mathscr{U}^{[0,T]} \; ; \quad \mathbf{u}_{|\partial_1\Omega} = \mathbf{U}_d \text{ on }]0, T[\tag{1}$$

- the equilibrium equations (principle of virtual work):

$$\sigma \in \mathscr{S}^{[0,T]} \; ; \forall t \in]0, T[\;\; \forall \mathbf{u}^* \in \mathscr{U}_{ad,0}$$
$$-\int_\Omega \sigma : \varepsilon(\mathbf{u}^*) \mathrm{d}\Omega + \int_\Omega \mathbf{f}_d \cdot \mathbf{u}^* \mathrm{d}\Omega + \int_{\partial_2\Omega} \mathbf{F}_d \cdot \mathbf{u}^* \mathrm{d}S = \int_\Omega \rho \frac{\mathrm{d}^2\mathbf{u}}{\mathrm{d}t^2} \cdot \mathbf{u}^* \mathrm{d}\Omega \tag{2}$$

- the constitutive relation:

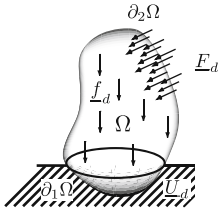

Fig. 1 Schematic representation of the environment (i.e. the prescribed conditions)

$$\forall t \in [0,T] \;\; \forall \mathbf{x} \in \Omega \quad \sigma_{|t} = \mathbf{A}\big(\varepsilon(\dot{\mathbf{u}}_{|\tau}); \tau \leq t\big) \tag{3}$$

$\varepsilon(\mathbf{u})$ denotes the strain associated with the displacement $\big(\varepsilon(\mathbf{u})_{ij} = \frac{1}{2}(u_{i,j} + u_{j,i})\big)$. $\mathscr{U}^{[0,T]}$ is the space containing the displacement field $\mathbf{u}$ defined over $\Omega \times]0,T[$, and $\mathscr{S}^{[0,T]}$ is the space containing the stresses, also defined over $\Omega \times]0,T[$. Finally, $\mathscr{U}_{ad,0}$ is the vector space of the prescribed virtual velocities. Operator $\mathbf{A}$, which is given and generally single-valued, characterizes the mechanical behavior of the material. ρ is the density.

In the following we denote $\mathscr{U}_{ad}^{[0,T]}$ the space of displacement fields which verify (1), and $\mathscr{S}_{ad}^{[0,T]}$ the space of stress fields which verify (2).

3 Use of CRE for Elasticity Problems

Let us start with the simplest family of mechanical problems, i.e. elasticity problems. We focus on the final state of the structure at $t = T$; thus, the problem to be solved does not depend on time. Moreover, the constitutive relation (3) becomes:

$$\sigma = \mathbf{K}\varepsilon(\mathbf{u}) \tag{4}$$

where $\mathbf{K}$ denotes the Hooke tensor, which is symmetric and positive definite. The densities $\mathbf{U}_d$, $\mathbf{f}_d$, and $\mathbf{F}_d$ are known at $t = T$. $\mathscr{U} = [H^1(\Omega)]^d$ and $\mathscr{S} = \{\text{second order symmetric tensor fields } \pi \in [L^2(\Omega)]^{d(d+1)/2}\}$. The spaces of the admissible displacements and stresses are $\mathscr{U}_{ad}$ and $\mathscr{S}_{ad}$, respectively.

3.1 Basics on CRE and Global Error Estimation

We assume that the finite element solution was calculated using a displacement approach. Thus, the finite element displacement-stress pair $(\mathbf{u}_h, \sigma_h)$ is known and the stress σ_h is FE-equilibrated.

The principle behind our approach consists in associating a new and admissible displacement-stress pair (i.e. belonging to $\mathscr{U}_{ad} \times \mathscr{S}_{ad}$), denoted $(\hat{\mathbf{u}}_h, \hat{\sigma}_h)$, to the data and the finite element displacement-stress pair. This new entity also verifies what we call the *prolongation conditions*, which are relations with the finite element solution. The construction of $(\hat{\mathbf{u}}_h, \hat{\sigma}_h)$ is achieved through a general quasi-explicit technique which is now well-known [4, 34, 35], and which has several recent variants [26, 36]; an overview is given in the Appendix. For the displacement field, we generally take $\hat{\mathbf{u}}_h = \mathbf{u}_h$; for quasi-incompressible materials, a modification is shown in [37].

Let us first recall the Prager-Synge theorem [4, 38] which links the constitutive relation error to the error in the solution. Introducing the constitutive relation error:

$$[E^h_{CRE}]^2 \equiv \Phi^*(\hat{\sigma}_h) + \Phi(\hat{\varepsilon}_h) - \int_\Omega \hat{\sigma}_h : \hat{\varepsilon}_h \mathrm{d}\Omega \quad \text{with} \quad \hat{\varepsilon}_h \equiv \varepsilon(\hat{\mathbf{u}}_h) \tag{5}$$

where Φ and Φ^* are the global potentials (dual convex functions) of the constitutive relation:

$$\begin{aligned} \Phi^*(\sigma) &\equiv \int_\Omega \varphi^*(\sigma)\mathrm{d}\Omega \quad ; \quad \varphi^*(\sigma) \equiv \frac{1}{2}\sigma : \mathbf{K}^{-1}\sigma \\ \Phi(\varepsilon) &\equiv \int_\Omega \varphi(\varepsilon)\mathrm{d}\Omega \quad ; \quad \varphi(\varepsilon) \equiv \frac{1}{2}\varepsilon : \mathbf{K}\varepsilon \end{aligned} \tag{6}$$

we have the following properties:

$$\begin{aligned} \Phi^*(\sigma - \hat{\sigma}_h) + \Phi(\varepsilon - \hat{\varepsilon}_h) &= [E^h_{CRE}]^2 \\ \Phi^*(\sigma - \hat{\sigma}_{h,m}) &= \frac{1}{4}[E^h_{CRE}]^2 \quad \text{with} \quad \hat{\sigma}_{h,m} \equiv \frac{1}{2}\left[\hat{\sigma}_h + \mathbf{K}\hat{\varepsilon}_h\right] \end{aligned} \tag{7}$$

The first relation in (7) leads to the guaranteed upper bound $||\mathbf{u} - \mathbf{u}_h||_\mathbf{K} \leq \sqrt{2}E^h_{CRE}(\mathbf{u}_h, \hat{\sigma}_h)$ on the global discretization error (in the energy norm $||\bullet||_\mathbf{K}$), and the quality of this bound depends on that of $\hat{\sigma}_h$. An illustration taken from [36] is given in Fig. 2 and exhibits the distribution of the error estimate $\sqrt{2}E^h_{CRE}(\mathbf{u}_h, \hat{\sigma}_h)$ over the elements of the mesh. The structure is clamped on part of its boundary and subjected to unit traction forces on the opposite boundary. The elastic material is isotropic and linear with $E = 1$ and $\nu = 0.3$.

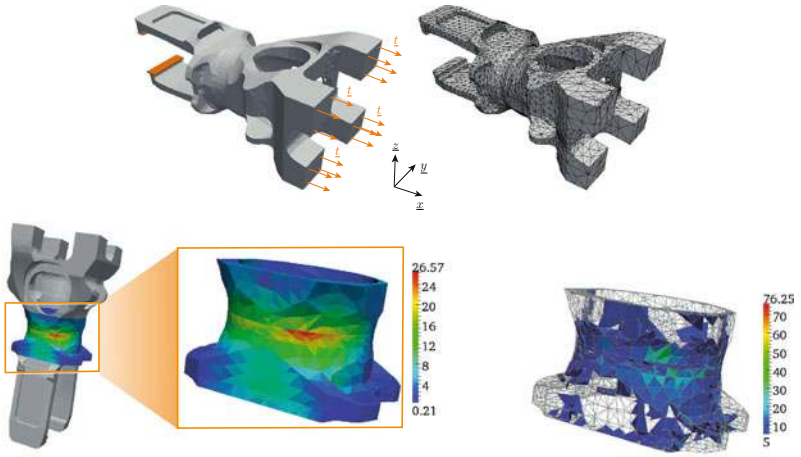

Fig. 2 Reference problem (*top left*) with associated FE mesh (*top right*), magnitude of the FE Von Mises stress (*bottom left*), and distribution of higher local contributions to the error (*bottom right*)

3.2 Goal-Oriented Error Estimation

We now consider a local measure of the discretization error, defined on an output of interest Q.

3.2.1 The Output of Interest

The quantity of interest Q is a goal-oriented quantity, such as the mean value of a stress or displacement component over an element or a set of elements. Such an output of interest can be written globally:

$$Q = \int_\Omega \sigma : \tilde{\Sigma} \mathrm{d}\Omega \tag{8}$$

where $\tilde{\Sigma}$ is the extractor which defines Q. Here, for the sake of simplicity, we do not consider convex nonlinear functionals of the stress, but such extensions would not involve serious difficulties. The Q-error is $|Q - Q_h|$ where Q_h is the value obtained from the finite element solution $(\mathbf{u}_h, \sigma_h)$.

In order to get a relevant bound on $|Q - Q_h|$, a common practice is to calculate what is called the adjoint problem, which is very classical in this case: it consists in an elasticity problem with a pre-strain $\tilde{\Sigma}$. Its finite element solution, which can be obtained with a refined mesh, is denoted $(\tilde{\mathbf{u}}_h, \tilde{\sigma}_h)$, and an associated admissible FE solution is $(\hat{\tilde{\mathbf{u}}}_h, \hat{\tilde{\sigma}}_h)$. The main result is [20]:

Theorem 1 *The following guaranteed upper bound holds:*

$$|Q - Q_h - Q_{corr}| \leq E^h_{CRE}.\tilde{E}^h_{CRE} \tag{9}$$

where E^h_{CRE} and $\tilde{E}^h_{CRE}$ are the constitutive relation errors related to the reference problem and the adjoint problem, respectively. Q_{corr} is a correction term defined as:

$$Q_{corr} \equiv \int_\Omega \left(\hat{\sigma}_h - \mathbf{K}\varepsilon(\hat{\mathbf{u}}_h)\right) : \mathbf{K}^{-1}\hat{\tilde{\sigma}}_{h,m} d\Omega + \int_\Omega \left(\mathbf{K}\varepsilon(\hat{\mathbf{u}}_h) - \sigma_h\right) : \tilde{\Sigma} d\Omega \tag{10}$$

Proof The adjoint problem is here the previous elasticity one, the structure being submitted to the pre-strain $\tilde{\Sigma}$; zero-value displacements and tractions are prescribed on the boundary $\partial\Omega$. The starting point is:

$$Q - Q_h = \int_\Omega \mathbf{K}\varepsilon(\mathbf{u} - \hat{\mathbf{u}}_h) : \tilde{\Sigma} \mathrm{d}\Omega + \int_\Omega \mathbf{K}\varepsilon(\hat{\mathbf{u}}_h - \mathbf{u}_h) : \tilde{\Sigma} \mathrm{d}\Omega \tag{11}$$

Noticing that:

$$\begin{aligned}\int_\Omega \mathbf{K}\varepsilon(\mathbf{u}-\hat{\mathbf{u}}_h) : \tilde{\Sigma}\mathrm{d}\Omega &= \int_\Omega \varepsilon(\mathbf{u}-\hat{\mathbf{u}}_h) : \mathbf{K}\varepsilon(\tilde{\mathbf{u}})\mathrm{d}\Omega \\ &= \int_\Omega \varepsilon(\mathbf{u}-\hat{\mathbf{u}}_h) : (\tilde{\sigma} - \mathbf{K}\varepsilon(\hat{\tilde{\mathbf{u}}}_h))\mathrm{d}\Omega + \int_\Omega \varepsilon(\mathbf{u}-\hat{\mathbf{u}}_h) : \mathbf{K}\varepsilon(\hat{\tilde{\mathbf{u}}}_h)\mathrm{d}\Omega \quad (12) \\ &= \int_\Omega \varepsilon(\mathbf{u}-\hat{\mathbf{u}}_h) : (\hat{\tilde{\sigma}}_h - \mathbf{K}\varepsilon(\hat{\tilde{\mathbf{u}}}_h))\mathrm{d}\Omega + \int_\Omega (\hat{\sigma}_h - \mathbf{K}\varepsilon(\hat{\mathbf{u}}_h)) : \varepsilon(\hat{\tilde{\mathbf{u}}}_h)\mathrm{d}\Omega\end{aligned}$$

and introducing $\hat{\sigma}_{h,m}$ and $\hat{\tilde{\sigma}}_{h,m}$ as in (7), we get $Q - Q_h - Q_{corr} = \int_\Omega \left(\sigma - \hat{\sigma}_{h,m}\right) : \mathbf{K}^{-1}\left(\hat{\tilde{\sigma}}_h - \mathbf{K}\varepsilon(\hat{\tilde{\mathbf{u}}}_h)\right)\mathrm{d}\Omega$. Using the Cauchy-Schwarz inequality and (7), we obtain the final upper bound.

Remark 1 The bound defined by the second member of (9) is half of the classical bound (see [4]). Indeed, introducing $\hat{\sigma}_{h,m}$ enables a more accurate bounding.

Remark 2 The value of the calculated error bound depends on the meshes used to solve the reference and adjoint problems. It is always possible, by refining the mesh of the adjoint problem alone, to control the value of the Q-error. In general, a local refinement (near the domain of interest) of the mesh used to solve the adjoint problem is very effective [23, 33].

Remark 3 The Galerkin orthogonality property related to the FE solution is not used to derive Theorem 1.

Remark 4 Theorem 1 is based on the Cauchy-Schwarz inequality as nearly all error bounds. In [27], a new bounding technique using the Saint-Venant principle and homothetic domains is derived; this can give sharper bounds. The idea is to decompose the domain Ω in two disjoint zones: (i) zone ω_λ, parameterized with scalar value λ, surrounding the zone where the quantity of interest is defined; (ii) complementary zone Ω/ω_λ. We can then write $Q - Q_h - Q_{corr} = q_{\omega_\lambda} + q_{\Omega/\omega_\lambda}$.

Bounding the term $q_{\Omega/\omega_\lambda}$ can be easily and accurately performed from the Cauchy-Schwarz inequality applied over Ω/ω_λ, as $\tilde{E}^h_{CRE|\Omega/\omega_\lambda}$ remains small in practice. Bounding the other term q_{ω_λ} is more technical; it leans on an inequality, related to Saint-Venant's principle, of the form:

$$||\sigma - \hat{\sigma}_h||_{\mathbf{K}^{-1}|\omega_\lambda} \leq \left(\frac{\lambda}{\overline{\lambda}}\right)^{1/k} ||\sigma - \hat{\sigma}_h||_{\mathbf{K}^{-1}|\omega_{\overline{\lambda}}} + \gamma_{\lambda,\overline{\lambda}} \quad (13)$$

where $\omega_{\overline{\lambda}}$ is a homothetic domain of ω_λ, parameterized by scalar value $\overline{\lambda} \geq \lambda$ (Fig. 3), k is a computable constant that depends on the geometry of ω_λ (and obtained analytically or numerically by solving an additional local eigenvalue problem), and $\gamma_{\lambda,\overline{\lambda}}$ is a known term. In practice, $\overline{\lambda}$ is chosen the highest possible while ensuring $\omega_{\overline{\lambda}} \subset \Omega$, and λ the smallest possible with ω_λ surrounding the zone of interest. The exponential decrease with respect to $\lambda/\overline{\lambda}$ in (13) is the key point to avoid overestimation.

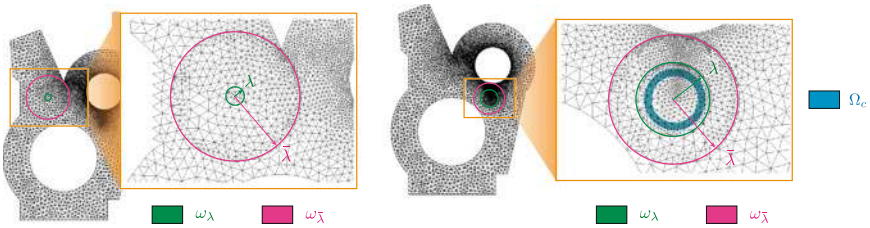

Fig. 3 Homothetic domains ω_λ and $\omega_{\bar{\lambda}}$ defined in a cracked structure when considering different quantities of interest: local mean of a component of σ (*left*), and stress intensity factors in the vicinity of the crack (*right*)

4 Use of CRE for Visco-Plasticity Problems

4.1 Basics on CRE and Global Error Estimation

We rewrite the reference problem (1)–(3) using some global notations within the framework of classical thermodynamics with internal variables. Let us introduce the following generalized quantities:

$$s = \begin{bmatrix} \sigma \\ \mathbf{Y} \end{bmatrix} \qquad \dot{e}_p = \begin{bmatrix} \dot{\varepsilon}_p \\ -\dot{\mathbf{X}} \end{bmatrix} \qquad \dot{e}_e = \begin{bmatrix} \dot{\varepsilon}_e \\ \dot{\mathbf{X}} \end{bmatrix} \tag{14}$$

where additional internal variables are gathered in the n-vectors $\mathbf{X}$ and $\mathbf{Y}$. The dissipation bilinear form over the time-space domain is:

$$(\dot{e}_p, s) \longmapsto \int_0^T \int_\Omega s \cdot \dot{e}_p \, \mathrm{d}\Omega \, \mathrm{d}t = \int_0^T \int_\Omega \left(\sigma : \dot{\varepsilon}_p - \mathbf{Y} \cdot \dot{\mathbf{X}}\right) \mathrm{d}\Omega \, \mathrm{d}t \tag{15}$$

The reference problem is thus to find $(\dot{e}_p, s) \in \mathscr{S}^{[0,T]}$ such that:

$$\begin{aligned} &\bullet\ \dot{e} = \dot{e}_e + \dot{e}_p \text{ is kinematically admissible} \\ &\bullet\ s \text{ is statically admissible} \\ &\bullet\ e_e = \boldsymbol{\Lambda}(s) \quad \text{(state equations)} \\ &\bullet\ \dot{e}_p = \mathbf{B}(s) \quad \text{(evolution laws)} \\ &\bullet\ s = 0, e = 0 \text{ at } t = 0 \quad \text{(initial conditions)} \end{aligned} \tag{16}$$

$\boldsymbol{\Lambda}$ is assumed to be linear; most viscoplastic materials are in this category (see [3, 39]) and this material description is called *normal*. $\mathbf{B}$ could be nonlinear and multivalued, as in plasticity, but here we consider the family of standard materials whose state evolution laws can be expressed with two potentials, which are dual (in the Legendre-Fenchel sense) convex functions φ and φ^* such that for $(t, \mathbf{x}) \in [0, T] \times \Omega$:

$$\forall(\dot{e}_p, s) \in \mathscr{S}^{[0,T]} \quad \varphi^*(s) + \varphi(\dot{e}_p) - s \cdot \dot{e}_p \geq 0$$
$$\varphi^*(s) + \varphi(\dot{e}_p) - s \cdot \dot{e}_p = 0 \Longleftrightarrow \dot{e}_p = \mathbf{B}(s) \tag{17}$$

Then, the constitutive relation (dissipation) error related to $(\dot{e}_p, s) \in \mathscr{S}^{[0,T]}$ is:

$$[E_{CRE}]^2 = \int_0^T \int_\Omega \left[\varphi^*(s) + \varphi(\dot{e}_p) - s \cdot \dot{e}_p\right] \mathrm{d}\Omega \, \mathrm{d}t \tag{18}$$

4.1.1 The Associated Admissible FE Solution

In the dissipation error framework, the concept of admissibility must be modified [3]:

Definition 1 A pair $(\dot{e}_p, s) \in \mathscr{S}^{[0,T]}$ is admissible if:
(i) the state equations are verified $\left(e_e = \boldsymbol{\Lambda}(s)\right)$
(ii) $\dot{e} = \dot{e}_e + \dot{e}_p$ and s verify the kinematic constraints and the equilibrium equations.

To go further, let us assume that the calculated solution was obtained using the FE method. Thus, at discrete time points t_m belonging to $[0, T]$, we know:

$$[\dot{e}_h, s_h]_t \quad ; \quad t \in [0, t_1, \ldots, t_n = T] \tag{19}$$

and $[\dot{e}_h, s_h]_t$ verifies the kinematic constraints and equilibrium equations in the FE sense at these discrete time points. Assuming that the evolution of the data during each time step is linear, we can extend the FE solution across the whole time-space domain. Thus, we get $(\dot{e}_h, s_h) \in \mathscr{S}^{[0,T]}$ which verifies the kinematic constraints and the equilibrium equations in the FE sense at any time $t \in [0, T]$.

In order to get an associated admissible solution, we use the same technique as in elasticity to define a displacement-stress pair $(\hat{\mathbf{u}}_h, \hat{\sigma}_h)$ which is admissible in the classical sense i.e. which verifies the kinematic constraints, the equilibrium equations and the initial conditions over $[0, T] \times \Omega$. Let us note that in the case of (visco-)plasticity with the constraint $\mathrm{Tr}[\dot{\varepsilon}_p] = 0$, the previous displacement must be modified so that $\mathrm{Tr}[\dot{\hat{\varepsilon}}_p] = 0$. The additional internal variables $(\hat{\mathbf{X}}_h, \hat{\mathbf{Y}}_h)$ which must verify the state equations can be easily constructed by solving local problems related to the minimization of the constitutive relation error of the dissipation type. Finally, we obtain an admissible solution $(\dot{\hat{e}}_p, \hat{s}) \in \mathscr{S}^{[0,T]}$ of the reference model. More details can be found in [4, 39].

The differences between the computerized structural model and the reference model are not limited to numerical aspects like time and space discretizations; models can differ in their state evolution laws. For example, the reference can be a viscoplastic material model while the calculations are performed with an elastic model.

4.1.2 Link Between the Constitutive Relation Error and the Error in the Solution

Let us first introduce what we call the φ-tangent potential at x:

$$\overline{\varphi}(x' - x) \equiv \varphi(x') - \varphi(x) - y \cdot (x' - x) \geq 0 \tag{20}$$

where φ, φ^* are two dual convex functions and (x, y) is such that $\varphi(x) + \varphi^*(y) - x \cdot y = 0$; $\overline{\varphi} = \varphi$ for quadratic potentials. We give a new version of the fundamental link between the constitutive relation error and the error in the solution derived in [3]:

Theorem 2 *Let $(\dot{e}_p, s)$ be the exact solution and $(\dot{\hat{e}}_{p,h}, \hat{s}_h)$ an arbitrary admissible solution to the reference problem. We have:*

$$\overline{\Phi}^*\big(s - \mathbf{B}^{-1}(\dot{\hat{e}}_{p,h})\big) + \overline{\Phi}\big(\dot{e}_p - \mathbf{B}(\hat{s}_h)\big) + \int_0^T |\dot{a}| E_F(s - \hat{s}_h) dt = [E^h_{CRE}]^2 \tag{21}$$

$$\begin{aligned} \textit{with}: &\bullet\ \overline{\Phi} \equiv \int_0^T \int_\Omega a(t)\overline{\varphi}\ d\Omega\ dt \qquad \overline{\Phi}^* \equiv \int_0^T \int_\Omega a(t)\overline{\varphi}^* d\Omega\ dt \\ &\bullet\ [E^h_{CRE}]^2 = \int_0^T \int_\Omega a(t)\Big[\varphi^*(\hat{s}_h) + \varphi(\dot{\hat{e}}_{p,h}) - \hat{s}_h \cdot \dot{\hat{e}}_{p,h}\Big] d\Omega\ dt \\ &\bullet\ E_F : \textit{free energy} \\ &\bullet\ a(t) : \textit{arbitrary function such that}\ \ a(t) \geq 0\ \ \dot{a} \leq 0\ \ a(T) = 0 \end{aligned} \tag{22}$$

In some applications, it is interesting to restrict the time interval to a subinterval $[T', T]$. An identity similar to (21) holds, with the additional term $a(T')E^+_{F|T'}$ on the right-hand side, where E^+_F is an upper bound on $E_F(s - \hat{s}_h)_{|T'}$.

Proposition 1 *An upper bound on the free energy $E_F(s - \hat{s}_h)$ at t is $E^+_F(t)$, solution to:*

$$E^+_F(0) = 0\ \ ;\ \ \frac{d}{dt}(E^+_F) + \omega(E^+_F, t) = \int_\Omega \Big[\varphi^*(\hat{s}_h) + \varphi(\dot{\hat{e}}_{p,h}) - \hat{s}_h \cdot \dot{\hat{e}}_{p,h}\Big] d\Omega \tag{23}$$

where ω is a function such that:

$$\omega\big(E^+_F(\Delta s), t\big) \leq \inf_{\Delta s \in \mathcal{S}_{ad,0}} \int_\Omega \Big[\overline{\varphi}^*\big(\Delta s + \hat{s}_h - \mathbf{B}^{-1}(\dot{\hat{e}}_{p,h})\big) + \overline{\varphi}\big(\mathbf{B}(\Delta s + \hat{s}_h) - \mathbf{B}(\hat{s}_h)\big)\Big] d\Omega \tag{24}$$

$\mathcal{S}_{ad,0}$ being the space of statically admissible generalized stress fields under homogeneous conditions.

The proof of Proposition 1 essentially uses Theorem 2, written locally in time.

4.2 Goal-Oriented Error Estimation

The output of interest can be defined as:

$$Q = \int_0^T \int_\Omega \left[\sigma : \delta\dot{\tilde{\Sigma}} - \mathbf{Y} \cdot \delta\dot{\tilde{\mathbf{X}}}\right] \mathrm{d}\Omega \, \mathrm{d}t = \int_0^T \int_\Omega s \cdot \delta\dot{\tilde{e}}_\Sigma \, \mathrm{d}\Omega \, \mathrm{d}t \tag{25}$$

where the extractor is $\delta\dot{\tilde{e}}_\Sigma = \begin{bmatrix} \delta\dot{\tilde{\Sigma}} \\ -\delta\dot{\tilde{\mathbf{X}}} \end{bmatrix}$ with $\delta\dot{\tilde{e}}_\Sigma = 0$ at $t = T$.

Here, δ is a symbol indicating that $\delta\dot{\tilde{e}}_\Sigma$ must be interpreted as a finite, but relatively small, variation. *However, we do not carry out any linearization*. The classical adjoint problem is replaced by what we call the *mirror* problem, which is similar to the reference problem except that time goes backwards: $\tau \equiv T - t$. This mirror problem, written with δ-quantities, is defined as:

Find $(\delta\dot{\tilde{e}}_p, \delta\tilde{s}) \in \mathscr{S}^{[0,T]}$ such that:

$$\begin{aligned}
&\bullet\ \delta\dot{\tilde{e}} = \delta\dot{\tilde{e}}_e + \delta\dot{\tilde{e}}_p \text{ is kinematically admissible} \\
&\bullet\ \delta\tilde{s} - \delta\tilde{s}_\Sigma \text{ is statically admissible} \\
&\bullet\ \delta\tilde{e}_e = \boldsymbol{\Lambda}(\delta\tilde{s}) \quad \text{(state equations)} \\
&\bullet\ \delta\dot{\tilde{e}}_p = \tilde{\mathbf{B}}(\delta\tilde{s}) \equiv \boldsymbol{B}(s_h + \delta\tilde{s}) - \mathbf{B}(s_h) \quad \text{(evolution laws)} \\
&\bullet\ \delta\tilde{s} = 0, \delta\dot{\tilde{e}} = 0 \text{ at } \tau = 0 \quad \text{(initial conditions)}
\end{aligned} \tag{26}$$

where $s_h(\tau)$ is the FE solution to the reference problem and $\delta\dot{\tilde{e}}_\Sigma = \tilde{\mathbf{B}}(\delta\tilde{s}_\Sigma) + \boldsymbol{\Lambda}(\delta\dot{\tilde{s}}_\Sigma)$.

Let $(\dot{\tilde{e}}_h, \tilde{s}_h)$ be the FE solution to the mirror problem and $(\dot{\hat{\tilde{e}}}_h, \hat{\tilde{s}}_h)$ the associated admissible FE solution over $[0, T] \times \Omega$. From now on, all these quantities will be defined with respect to the initial time t.

4.2.1 Upper Error Bound for an Output of Interest

The starting point is the following relation, which can be easily proven.

Proposition 2 *Using the previous notations, the Q-error is equal to:*

$$-Q + Q_h + Q_{corr} = \int_0^T \int_\Omega \left(s - \hat{s}_{h,m}\right) \cdot \left(\tilde{\mathbf{B}}(\delta\hat{\tilde{s}}_h) - \delta\dot{\hat{\tilde{e}}}_{p,h}\right) d\Omega \, dt + \mathbf{C}(s - s_h, \delta\tilde{s}_\Sigma) - \mathbf{C}(s - s_h, \delta\hat{\tilde{s}}_h) \tag{27}$$

$$
\begin{aligned}
where: \bullet\ Q_{corr} \equiv & -\int_0^T \int_\Omega \Big[\big(\dot{\hat{e}}_h - \dot{e}_h\big) \cdot \big(\delta\tilde{s}_\Sigma - \delta\hat{\tilde{s}}_h\big) - \big(\hat{s}_h - s_h\big) \cdot \delta\dot{\hat{\tilde{e}}}_h \\
& + \big(\hat{s}_{h,m} - s_h\big) \cdot \big(\tilde{\mathbf{B}}(\delta\hat{\tilde{s}}_h) - \delta\dot{\hat{\tilde{e}}}_{p,h}\big) \Big] d\Omega\ dt \\
& \bullet\ \dot{e}_h = \boldsymbol{\Lambda}(\dot{s}_h) + \mathbf{B}(s_h) \quad ; \quad \delta\dot{\hat{\tilde{e}}}_{p,h|t} = \big[\delta\tilde{e}_{h,\tau} - \boldsymbol{\Lambda}(\delta\hat{\tilde{s}}_{h,\tau})\big]_{|\tau=T-t} \\
& \bullet\ \mathbf{C}(\Delta s, \delta s) = \int_0^T \int_\Omega [\Delta s \cdot \delta\dot{e}_p - \Delta\dot{e}_p \cdot \delta s] d\Omega\ dt \quad with \quad \Delta\dot{e}_p = \tilde{\mathbf{B}}(\Delta s)
\end{aligned}
\tag{28}
$$

Remark 5 The idea behind this relation is related to the **C**-terms: these are very small if the finite variations $(s - s_h)$ and $\delta\tilde{s}_\Sigma$ are small. Moreover, if the material model is linear, the **C**-terms are equal to zero. **C** is called the *model nonlinearity indicator*.

Remark 6 The generalized stress $\hat{s}_{h,m}$ is similar to the mean stress introduced in (7). In practice, we take an approximation of the minimization problem related to the cost function g:

$$
g(s - \hat{s}_{h,m}) = \int_0^T \Big[a\,\overline{\varphi}^*\big(s - \mathbf{B}^{-1}(\dot{\hat{e}}_{p,h})\big) + a\,\overline{\varphi}\big(\mathbf{B}(s) - \mathbf{B}(\hat{s}_h)\big) + |\dot{a}| E_F(s - \hat{s}_h) \Big] \mathrm{d}t \tag{29}
$$

Remark 7 The Galerkin orthogonality conditions related to the FE solution are not used.

We now derive upper bounds on the two terms in the right-hand side of (27). We only give the results here, but more details can be found in [20, 29].

Proposition 3 *Let be* $I_1 = \int_0^T \int_\Omega \big(s - \hat{s}_{h,m}\big) \cdot \big(\tilde{\mathbf{B}}(\delta\hat{\tilde{s}}_h) - \delta\dot{\hat{\tilde{e}}}_{p,h}\big) d\Omega\ dt$. *We have:*

$$
I_1 \leq 2\Big[[E^h_{CRE}]^2 - [E^h_{CRE,m}]^2 \Big]^{\frac{1}{2}} \cdot \Big[F^2(\overline{\mu}\,\dot{\tilde{a}}_h) \Big]^{\frac{1}{2}} + F^1(\dot{\tilde{a}}_h) \tag{30}
$$

$$
\begin{aligned}
with: \bullet\ & [E^h_{CRE,m}]^2 = \int_\Omega [\min_{y \in \mathscr{F}^{[0,T]}} g(y)] d\Omega \qquad \dot{\tilde{a}}_h = \tilde{\mathbf{B}}(\delta\hat{\tilde{s}}_h) - \delta\dot{\hat{\tilde{e}}}_h \\
& \bullet\ f(\dot{x}) \equiv \sup_{y \in \mathscr{F}^{[0,T]}} \Big[\int_0^T y \cdot \dot{x}\ dt - g(y) \Big] \quad \forall \dot{x} \in \mathscr{E}^{[0,T]} \quad \textit{(Legendre-Fenchel transform of } g\textit{)} \\
& \bullet\ f(\mu\,\dot{x}) = f(0) + \mu f^1(\dot{x}) + f^2(\mu\,\dot{x}) \quad with\ \mu \geq 0 \ \lim_{\mu \to 0^+} \frac{f^2(\mu\,\dot{x})}{\mu} = 0 \\
& \bullet\ F(\cdot) = \int_\Omega f(\cdot) d\Omega \qquad 1 = \frac{\big[[E^h_{CRE}]^2 - [E^h_{CRE,m}]^2\big]}{F^2(\overline{\mu}\,\dot{\tilde{a}}_h)}
\end{aligned}
\tag{31}
$$

An alternative bound for I_1 consists in using the Legendre-Fenchel transform for the dissipation bilinear form written at $(t, \mathbf{x}) \in [0, T] \times \Omega$. This bound is easier to obtain, but it is less effective. Another option is to work globally over $[0, T] \times \Omega$.

Let us now consider $I_2 \equiv \mathbf{C}(s - s_h, \delta\tilde{s}_\Sigma) - \mathbf{C}(s - s_h, \delta\hat{s}_h)$. We introduce $g_\Delta(\Delta s) \equiv g(\Delta s + \hat{s}_{h,m} - s_h)$ and define analytically, or at least numerically:

$$f_\Delta(\dot{a}, -b) = \sup_{\substack{\Delta s \in \mathscr{F}^{[0,T]} \\ \Delta\dot{e}_p = \tilde{\mathbf{B}}(\Delta s)}} \int_0^T \left[\Delta s \cdot \dot{a} - \Delta\dot{e}_p \cdot b - g_\Delta(\Delta s)\right] \mathrm{d}t \tag{32}$$

Writing $F_\Delta(\mu\delta\dot{\tilde{a}}, -\mu\delta\tilde{b}) = F_\Delta(0,0) + \mu F^1_\Delta(\delta\dot{\tilde{a}}, -\delta\tilde{b}) + F^2_\Delta(\mu\delta\dot{\tilde{a}}, -\mu\delta\tilde{b})$, the following bound can be proved:

$$I_2 \leq \left[[E^h_{CRE}]^2 - [E^h_{CRE,m}]^2\right]^{\frac{1}{2}} \left[F^2_\Delta(\overline{\mu}\delta\dot{\tilde{a}}, -\overline{\mu}\delta\tilde{b})\right]^{\frac{1}{2}} + F^1_\Delta(\delta\dot{\tilde{a}}, -\delta\tilde{b}) \quad ; \quad 1 = \frac{\left[[E^h_{CRE}]^2 - [E^h_{CRE,m}]^2\right]}{F^2_\Delta(\overline{\mu}\delta\dot{\tilde{a}}, -\overline{\mu}\delta\tilde{b})} \tag{33}$$

F_Δ is small if the finite variations Δs and δs are small. A similar technique can be derived to get a strict lower bound.

Finally, from previous results, we obtain strict upper bounds on $|Q - Q_h - Q_{corr}|$. Illustrations of such bounds can be found in the literature: viscoelasticity (taking history effects into account) was addressed in [23], dynamics problems were considered in [22, 31], and nonlinear viscoplasticity problems were studied in [21]. Furthermore, the general case where the material operator $\mathbf{B}$ is not defined using two dual potentials (convex functions) but is simply maximum monotonous is given in [29].

In the following section, we focus on some recent advances for the computation of both accurate and practical bounds, in addition to be guaranteed, using the CRE framework.

5 Getting Accurate and Practical Error Bounds on Outputs of Interest

5.1 Non-intrusive Approach for the Adjoint Solution

As noticed in Sect. 3.2, the accuracy of the error bounds on Q can be controlled solving the adjoint problem with a locally refined mesh. However, this has the drawback to require remeshing of the structure. An alternative, qualified as non-intrusive as the initial mesh is not changed, was proposed in [24, 25]. It consists in a local enrichment of the adjoint solution, using PUM, with known *handbook* functions that aim at representing the high gradient part of $(\tilde{\mathbf{u}}, \tilde{\sigma})$; the approach is thus similar to that proposed in XFEM or GFEM [40, 41] except that no additional dof is introduced here (the singularity comes from the adjoint loading). We present the method in the linear elasticity case, but extensions to time-dependent problems can be found in [22, 24].

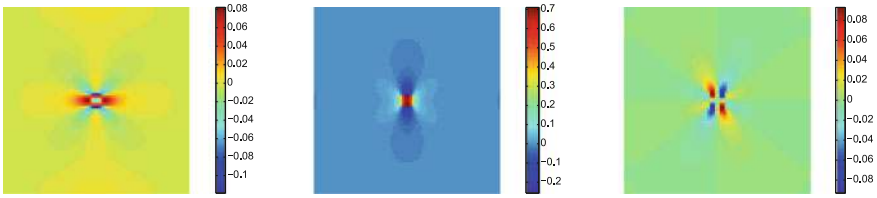

Fig. 4 Quasi-exact stress field in a (quasi-) infinite domain subjected to a local prestress in a squared region: $\tilde{\sigma}_{xx}^{hand}$ (*left*), $\tilde{\sigma}_{yy}^{hand}$ (*center*), $\tilde{\sigma}_{xy}^{hand}$ (*right*)

Enrichment functions which are used, denoted $(\tilde{\mathbf{u}}^{hand}, \tilde{\sigma}^{hand})$ in the following, correspond to generalized Green's functions and represent the (quasi-)exact adjoint solution in a (semi-)infinite domain subjected to the adjoint loading. These functions are obtained either analytically (when possible) or pre-computed numerically with a fine mesh an sufficiently large domain. An example of such a function, corresponding to a localized prestress loading $\tilde{\sigma}_\Sigma$, is given on Fig. 4. *Handbook* functions are inserted in the adjoint solution using the partition of unity defined by linear FE shape functions N_i associated to vertices i of the initial mesh ($N_i(\mathbf{x}_j) = \delta_{ij}$). The enrichment is introduced locally, and consequently only a set of n^{PUM} vertices are used. The enrichment region $\Omega^{PUM} \subset \Omega$ is defined as $\{\mathbf{x} \in \Omega, \sum_{i=1}^{n^{PUM}} N_i(\mathbf{x}) \neq 0\}$; it can be divided in two disjoint subregions Ω_1^{PUM} and Ω_2^{PUM} such that:

$$\sum_{i=1}^{n^{PUM}} N_i(\mathbf{x}) = \begin{cases} 1 & \text{in } \Omega_1^{PUM} \\ a \in]0,1[& \text{in } \Omega_2^{PUM} \\ 0 & \text{in } \Omega / (\overline{\Omega_1^{PUM} \cup \Omega_2^{PUM}}) \end{cases} \tag{34}$$

In practice, Ω_1^{PUM} is such that it contains the zone of interest Ω_Σ in which quantity Q is defined, i.e. the region that supports extraction functions.

Therefore, the displacement solution to the adjoint problem is searched under the form:

$$\tilde{\mathbf{u}}(\mathbf{x}) = \sum_{i=1}^{n^{PUM}} \tilde{\mathbf{u}}^{hand}(\mathbf{x}) N_i(\mathbf{x}) + \tilde{\mathbf{u}}^{res}(\mathbf{x}) \tag{35}$$

where $\tilde{\mathbf{u}}^{res}$ is a residual solution, usually very regular, to be computed. The enrichment part $\sum_{i=1}^{n^{PUM}} \tilde{\mathbf{u}}^{hand} N_i$ enables to reproduce local high gradients of $\tilde{\mathbf{u}}$ whereas the residual part $\tilde{\mathbf{u}}^{res}$ enables to correct the enrichment part in order to verify boundary conditions of the adjoint problem on $\partial\Omega$. The new expression of $\tilde{\sigma}$ is deducted from (35):

$$\tilde{\sigma}(\mathbf{x}) = \tilde{\sigma}_{PUM}^{hand}(\mathbf{x}) + \tilde{\sigma}^{res}(\mathbf{x}) \tag{36}$$

with $\tilde{\sigma}_{PUM}^{hand} = \mathbf{K}\varepsilon(\sum_{i=1}^{n^{PUM}} \tilde{\mathbf{u}}^{hand} N_i)$ and $\tilde{\sigma}^{res} = \mathbf{K}\varepsilon(\tilde{\mathbf{u}}^{res})$; of course, $\tilde{\sigma}_{PUM}^{hand} = \tilde{\sigma}^{hand}$ in Ω_1^{PUM}.

Once the set of n^{PUM} enriched vertices are defined, the new adjoint problem consists in finding $\tilde{\mathbf{u}}^{res} \in \mathscr{U}_{ad,0}$ such that:

$$a(\mathbf{v}, \tilde{\mathbf{u}}^{res}) = Q(\mathbf{v}) - a(\mathbf{v}, \sum_{i=1}^{n^{PUM}} \tilde{\mathbf{u}}^{hand} N_i) \quad \forall \mathbf{v} \in \mathscr{U}_{ad,0} \tag{37}$$

The residual stress field $\tilde{\sigma}^{res} = \mathbf{K}\varepsilon(\tilde{\mathbf{u}}^{res})$ then verifies the following balance equation:

$$\begin{aligned} \int_\Omega \tilde{\sigma}^{res} : \varepsilon(\mathbf{v}) \mathrm{d}\Omega &= \int_\Omega \left(\tilde{\sigma}_\Sigma : \varepsilon(\mathbf{v}) + \tilde{\mathbf{f}}_\Sigma \cdot \mathbf{v} \right) \mathrm{d}\Omega - \int_\Omega \tilde{\sigma}^{hand}_{PUM} : \varepsilon(\mathbf{v}) \mathrm{d}\Omega \\ &= \int_{\Omega_1^{PUM}} \left(\tilde{\sigma}_\Sigma : \varepsilon(\mathbf{v}) + \tilde{\mathbf{f}}_\Sigma \cdot \mathbf{v} - \tilde{\sigma}^{hand} : \varepsilon(\mathbf{v}) \right) \mathrm{d}\Omega - \int_{\Omega_2^{PUM}} \tilde{\sigma}^{hand}_{PUM} : \varepsilon(\mathbf{v}) \mathrm{d}\Omega \\ &= - \int_{\partial\Omega_1^{PUM}} \tilde{\sigma}^{hand} \mathbf{n}_{12} \cdot \mathbf{v} \mathrm{d}S - \int_{\Omega_2^{PUM}} \tilde{\sigma}^{hand}_{PUM} : \varepsilon(\mathbf{v}) \mathrm{d}\Omega \quad \forall \mathbf{v} \in \mathscr{U}_{ad,0} \end{aligned} \tag{38}$$

where $\mathbf{n}_{12}$ is the outgoing normal from Ω_1^{PUM} to Ω_2^{PUM}. The loading consists in tractions $-\tilde{\sigma}^{hand}\mathbf{n}_{12}$ on $\partial\Omega_1^{PUM}$ and a prestress $-\tilde{\sigma}^{hand}_{PUM}$ in Ω_2^{PUM}.

A fine approximation $(\tilde{\mathbf{u}}_h^{res}, \tilde{\sigma}_h^{res})$ of the residual solution can be obtained with the initial mesh; the enrichment technique is thus non-intrusive in the sense where operators (stiffness matrix, mesh connectivities) defined for the primal problem can be reused without any change to solve the adjoint problem; only the loading has to be modified. The computation of an admissible stress field $\hat{\tilde{\sigma}}_h$ is also performed in a non-intrusive way: one first defines a stress field $\hat{\tilde{\sigma}}_h^{res}$ that verifies (38), with the same method as that used to compute $\hat{\sigma}_h$; we then get:

$$\hat{\tilde{\sigma}}_h(\mathbf{x}) = \tilde{\sigma}^{hand}_{PUM}(\mathbf{x}) + \hat{\tilde{\sigma}}_h^{res}(\mathbf{x}) \tag{39}$$

Eventually, we obtain the following bounding:

$$|Q - Q_h - Q_{corr}| \leq E^h_{CRE} . \tilde{E}^h_{CRE,res} \tag{40}$$

where the right-hand side is independent of the enrichment $(\tilde{\mathbf{u}}^{hand}, \tilde{\sigma}^{hand})$. In practice, the error on the residual solution $\tilde{E}^h_{CRE,res}$ is small, and (40) provides for very accurate bounds on the local error without remeshing.

5.2 Application to Pointwise Quantities

When considering a quantity of interest which is pointwise in space (and/or in time), the loading of the adjoint problem is defined from Dirac functions. Consequently, the corresponding adjoint solution is highly singular and possibly infinite energy;

consequently, it is useless to compute an approximate solution with the FEM. A classical alternative method consists in regularizing the quantity of interest, using for instance weighting functions (molifiers) [11], in order to preserve the regularity of the adjoint solution; the initial quantity of interest is then replaced with a weighted local average.

The non-intrusive enrichment technique presented previously enables, with direct extension, to consider the evaluation of the discretization error for truly pointwise quantities, without resorting to regularization. For that, Green functions have to be chosen as enrichment functions. Under some assumptions, these functions can be determined analytically in a (semi-)infinite domain [42, 43]; an example of such a function is given in Fig. 5. In more complex situations (anisotropic material for instance), Green functions can sometimes be obtained implicitly [44].

Bounding (40) is still valid for pointwise quantities Q and bounds can be calculated despite of the fact that $(\tilde{\mathbf{u}}^{hand}, \tilde{\sigma}^{hand})$ may be infinite energy; indeed, only the residual part $(\tilde{\mathbf{u}}_h^{res}, \hat{\tilde{\sigma}}_h^{res})$ of the admissible adjoint solution is used to obtain error bounds. Nevertheless, technical numerical tools (numerical integration) are required to compute Q_{corr} and the loading term of the adjoint problem that imply the singular *handbook* solution $(\tilde{\mathbf{u}}^{hand}, \tilde{\sigma}^{hand})$.

In [22], the non-intrusive approach was conducted for visco-elastodynamics problems. Dealing with the singularity of the adjoint solution in space and time was performed by means of a local enrichment with Green's function associated to Q. Such a function can be calculated in a (semi-)infinite medium from the correspondence principle and Laplace transform. It was shown that local error bounds deteriorate when the model tends to a pure elastodynamics model; in this case, the influence zone of the Green function occupies the whole domain Ω and one needs to represent correctly this function after reflection on the boundary $\partial\Omega$; when viscous effects are important, this zone remains localized as the magnitude rapidly tends to zero (see Fig. 6 where we observe wave fronts P and S without or with 20 % damping, with Dirac loading in space and time). Local error bounds also deteriorate when the quantity of interest becomes more and more localized in time; this illustrates that considering a pointwise quantity in time for dynamics problems does not make real sense.

Eventually, and in addition to the non-intrusive approach, a technique was introduced in [25] in order to conserve guaranteed error bounds on nonlinear pointwise

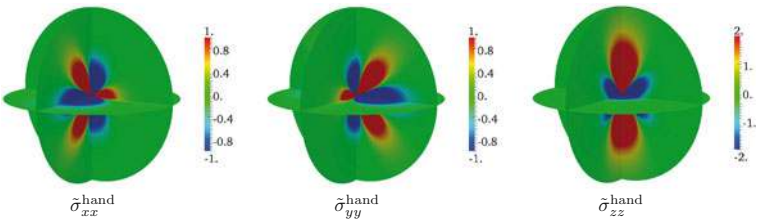

Fig. 5 Stress field associated to a pointwise prestress in a 3D infinite domain

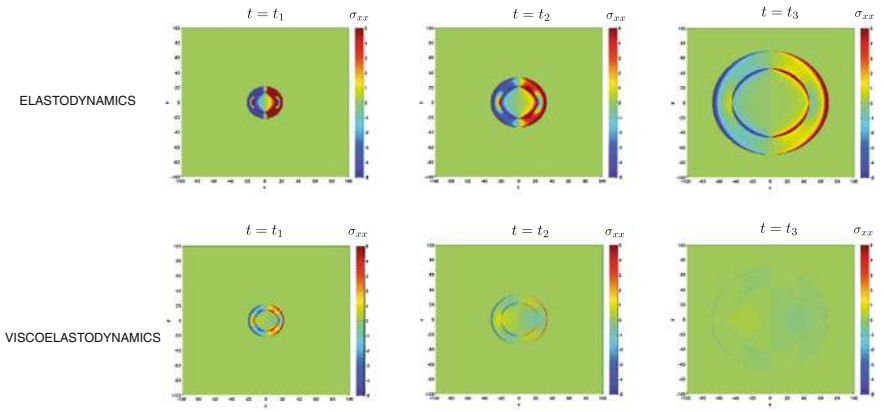

Fig. 6 Evolution of the xx component of *handbook* stress field for a model without (*top*) or with (*bottom*) damping

quantities of interest (such as the Von Mises equivalent stress). This technique is based on a decomposition of Q with projection properties in order to take higher order terms into account in the bounds. It leads to the introduction of a set of extractors, and therefore to the solution to a set of adjoint problems.

6 Control of Various Computational Approaches

6.1 Stochastic Approach

Currently, numerous models involving stochastic parameters are used to take hazards or lack of knowledge into account in numerical simulations. The verification of such models using the CRE concept has been investigated in [28, 45]; it requires: (i) the construction of admissible fields in a stochastic framework; (ii) the splitting between two error sources, coming from discretizations in the physical and stochastic spaces, in order to drive an adaptive process effectively.

Considering a linear elastic material with fluctuating properties, the Hooke tensor is modeled as a stochastic field $\mathbf{K}(\mathbf{x}, \theta) \in [L^2(\Theta, C^0(\Omega))]^{d^4}$; $(\Theta, \mathscr{F}, P)$ is the Kolmogorov probability space, with Θ the set of possible outcomes, $\mathscr{F}$ a σ-algebra of events (subspaces of Θ), and $P : \mathscr{F} \to [0, 1]$ a probability measure. We assume that field $\mathbf{K}(\mathbf{x}, \theta)$ is bounded and uniformly coercive, i.e. $\exists (K_{min}, K_{max}) \in]0, +\infty[^2$ such that:

$$0 < K_{min} \leq |\mathbf{K}(\mathbf{x}, \theta)| \leq K_{max} \quad \forall \mathbf{x} \in \Omega, \text{ almost surely} \tag{41}$$

In practice, following the Karhunen-Loeve decomposition, the stochastic description of $\mathbf{K}$ is restricted to a finite number M of independent stochastic variables $\xi_i(\theta) : \Theta \to \mathbb{R}$ such that:

$$\mathbf{K}(\mathbf{x},\theta) \approx \overline{\mathbf{K}}(\mathbf{x}) + \sum_{i=1}^{M} \sqrt{\lambda_i}\xi_i(\theta)\mathbf{Z}_i(\mathbf{x}) \tag{42}$$

where $\overline{\mathbf{K}}(\mathbf{x}) = \mathrm{E}_\Theta[\mathbf{K}(\mathbf{x})] = \int_\Theta \mathbf{K}(\mathbf{x})\mathrm{d}P$ is the mathematical expectation of $\mathbf{K}(\mathbf{x})$, whereas couples $\{\mathbf{Z}_i, \lambda_i\}$ are eigenvectors/eigenvalues of covariance operator associated to $\mathbf{K}$. We define the L^2 inner product $\langle \alpha_1(\theta), \alpha_2(\theta)\rangle \equiv \int_\Theta \alpha_1(\theta)\alpha_2(\theta)\mathrm{d}P$ over Θ, as well as following notations over $\Omega \times \Theta$:

$$\begin{aligned} \langle \mathbf{u}_1, \mathbf{u}_2\rangle_{\mathbf{K},\Theta} &= \mathrm{E}_\Theta\Big[\int_\Omega \mathbf{K}\varepsilon(\mathbf{u}_1) : \varepsilon(\mathbf{u}_2)\mathrm{d}\Omega\Big] \quad ; \quad ||\mathbf{u}||^2_{\mathbf{K},\Theta} = \langle \mathbf{u}, \mathbf{u}\rangle_{\mathbf{K},\Theta} \\ \langle \sigma_1, \sigma_2\rangle_{\mathbf{K}^{-1},\Theta} &= \mathrm{E}_\Theta\Big[\int_\Omega \mathbf{K}^{-1}\sigma_1 : \sigma_2\mathrm{d}\Omega\Big] \quad ; \quad ||\sigma||^2_{\mathbf{K}^{-1},\Theta} = \langle \sigma, \sigma\rangle_{\mathbf{K}^{-1},\Theta} \end{aligned} \tag{43}$$

Kinematic and static admissibility conditions thus respectively read:

$$\mathbf{u} \in \mathscr{U} \quad ; \quad \mathbf{u}_{|\partial_1\Omega} = \mathbf{u}_d \quad \text{almost surely} \tag{44}$$

$$\sigma \in \mathscr{S} \quad ; \quad \mathrm{E}_\Theta\left[\int_\Omega \sigma : \varepsilon(\mathbf{v})\mathrm{d}\Omega - \int_\Omega \mathbf{f}_d \cdot \mathbf{v}\mathrm{d}\Omega - \int_{\partial_2\Omega} \mathbf{F}_d \cdot \mathbf{v}\mathrm{d}S\right] = 0 \quad \forall \mathbf{v} \in \mathscr{U}_{ad,0} \tag{45}$$

with $\mathscr{U} = [L^2(\Theta, H^1(\Omega))]^d$ and $\mathscr{S} = \left\{\pi; \pi = \pi^T, \pi \in [L^2(\Theta, L^2(\Omega))]^{d^2}\right\}$. An approximate solution $(\mathbf{u}_{h,s}, \sigma_{h,s})$, with $\sigma_{h,s} = \mathbf{K}\varepsilon(\mathbf{u}_{h,s})$, is computed using FEM; without lost of generality, we consider here a non-intrusive technique on the stochastic domain, based on interpolation (discretization parameter s) of a set of computed realizations:

$$\mathbf{u}_{h,s}(\mathbf{x},\theta) = \sum_k \mathbf{u}^k_{h,s}(\mathbf{x}).\Psi_k(\theta) \quad ; \quad \sigma_{h,s}(\mathbf{x},\theta) = \sum_k \sigma^k_{h,s}(\mathbf{x}).\Psi_k(\theta) \tag{46}$$

where Ψ_k is a polynomial basis associated to the set $\{\xi_i(\theta)\}_{i=1}^M$ of stochastic variables, defined as $\Psi_k = \prod_{i=1}^M H_{k_i}(\xi_i)$ with $H_{k_i}(\xi_i)$ some orthogonal polynomials.

The definition of CRE in the stochastic framework:

$$E_{CRE}(\hat{\mathbf{u}}, \hat{\sigma}) = ||\hat{\sigma} - \mathbf{K}\varepsilon(\hat{\mathbf{u}})||_{\mathbf{K}^{-1},\Theta} \tag{47}$$

associated with an admissible solution in the sense of (44) and (45) enables to naturally extend properties of Sect. 3.1. An admissible solution $(\hat{\mathbf{u}}_{h,s}, \hat{\sigma}_{h,s})$ can be recovered by a post-processing of $(\mathbf{u}_{h,s}, \sigma_{h,s})$. In particular, from $\sigma^k_{h,s}(\mathbf{x})$, we can construct an associated equilibrated field $\hat{\sigma}^k_{h,s}(\mathbf{x})$ using the same techniques as those defined in the deterministic case [26, 36].

For goal-oriented error estimation, defining the output of interest in a global form:

$$Q = \mathrm{E}_\Theta \left[\int_\Omega \sigma : \tilde{\Sigma} \mathrm{d}\Omega \right] \tag{48}$$

we compute an approximate solution $(\tilde{\mathbf{u}}_{h,s}, \tilde{\sigma}_{h,s})$ of the associated (stochastic) adjoint problem, then an admissible solution. We thus get the following bound:

$$|Q - Q_{h,s} - Q_{corr}| \leq E^{h,s}_{CRE} . \tilde{E}^{h,s}_{CRE} \tag{49}$$

the proof of (49) being similar to the deterministic case. Another bounding consists in applying the Cauchy-Schwarz inequality over the space domain alone, before integrating over the stochastic dimension; the obtained bound is sharper but is more complex to compute.

The discretization error $Q - Q_{h,s}$ comes from two sources: (i) space discretization using a FE mesh; (ii) discretization of the stochastic domain. We can estimate the contribution of each source; indeed the local error can be recast as:

$$Q - Q_{h,s} = [Q - Q_h] + [Q_h - Q_{h,s}] = \Delta Q_{spa} + \Delta Q_{sto} \tag{50}$$

where ΔQ_{spa} (resp. ΔQ_{sto}) is the contribution to the local error due to discretization in the physical (resp. stochastic) space.

On the one hand, ΔQ_{sto} can be estimated with the CRE framework considering a semi-discretized reference model, already discretized in space (exact solution $\mathbf{u}_h$). In the sense of this new model, an admissible solution denoted $(\hat{\mathbf{u}}_s, \hat{\sigma}_s)$ is constructed from a post-processing of $(\mathbf{u}_{h,s}, \sigma_{h,s})$; in particular, $\hat{\sigma}_s$ should verify the FE equilibrium over Θ. A similar construction is used to construct an admissible solution $(\hat{\tilde{\mathbf{u}}}_s, \hat{\tilde{\sigma}}_s)$ for the adjoint problem. Consequently, ΔQ_{sto} can be assessed from the bound $E^s_{CRE} \cdot \tilde{E}^s_{CRE}$. On the other hand, $\Delta Q_{spa} \approx Q_s - Q_{h,s}$ can be assessed considering a semi-discretized reference problem, already discretized over the stochastic dimension (exact solution $\mathbf{u}_s$). An admissible solution denoted $(\hat{\mathbf{u}}_h, \hat{\sigma}_h)$ is constructed in the sense of this new model; in particular, $\hat{\sigma}_h$ should verify equilibrium for each computed realization in Θ. After computing a similar admissible solution $(\hat{\tilde{\mathbf{u}}}_h, \hat{\tilde{\sigma}}_h)$ for the adjoint problem, ΔQ_{spa} can be assessed from the bound $E^h_{CRE} \cdot \tilde{E}^h_{CRE}$.

6.1.1 XFEM Approach

We consider here the XFEM method in a two-dimensional setting. Introduced in [40] as a generalization of FEM, XFEM enables to capture local solution features in a cracked domain (Fig. 7). In order to improve the convergence rate and use a non-conforming mesh with respect to a crack Γ (supposed free of charge), the XFEM method consists in enriching the classical FE approximation by means of the partition

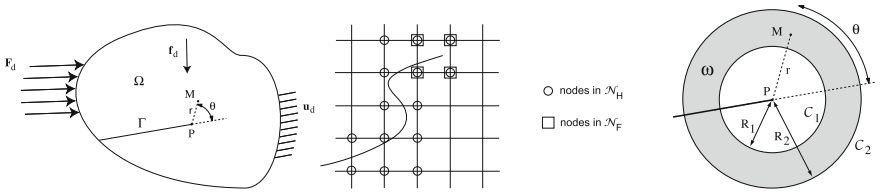

Fig. 7 2D cracked structure (*left*), sets $\mathcal{N}_H$ and $\mathcal{N}_F$ of enriched nodes in a regular mesh (*center*), and definition of the crown ω surrounding the crack tip (*right*)

of unity defined by shape functions $N_i(\mathbf{x})$, and implying two kinds of enrichment functions:

- the Heaviside function $H(\mathbf{x})$ that enables to represent displacement jumps across Γ. This function is ± 1 on the two edges of the crack and is in practice obtained with level-set functions. The enrichment with $H(\mathbf{x})$ is applied to the set $\mathcal{N}_H$ of nodes associated to elements which are cut by the crack (Fig. 7);
- the set $\{F_j(\mathbf{x}),\, 1 \leq j \leq 4\}$ of basis functions that generate the singular asymptotic solution in the vicinity of the crack tip P:

$$\left\{ \sqrt{r}\cos(\frac{\theta}{2}),\, \sqrt{r}\sin(\frac{\theta}{2}),\, \sqrt{r}\cos(\frac{\theta}{2})\sin(\frac{\theta}{2}),\, \sqrt{r}\sin(\frac{\theta}{2})\sin(\frac{\theta}{2}) \right\} \tag{51}$$

  Enrichment with functions $F_j(\mathbf{x})$ is applied to the set $\mathcal{N}_F$ of nodes associated to elements surrounding the crack tip (Fig. 7).

Therefore, noticing $\mathcal{N}$ the set of nodes in the mesh, the approximate XFEM displacement solution is searched under the form:

$$\mathbf{u}_h(\mathbf{x}) = \sum_{i \in \mathcal{N}} N_i(\mathbf{x})\mathbf{u}_i + \sum_{i \in \mathcal{N}_F} N_i(\mathbf{x}) \left(F_j(\mathbf{x})\mathbf{a}_i^j \right) + \sum_{i \in \mathcal{N}_H} N_i(\mathbf{x}) H(\mathbf{x}) \mathbf{b}_i \tag{52}$$

where $\{\mathbf{u}_i\}$ is the set of standard FE dofs whereas $\{\mathbf{a}_i^j, \mathbf{b}_i\}$ is the set of additional dofs.

In most cases, compared to classical FEM, the enrichment introduced by XFEM improves the accuracy of the approximate solution as well as values of related quantities of interest. Nevertheless, estimating the discretization error remains fundamental for robust computations. For fracture Mechanics, verification with respect to outputs of interest was addressed in [46, 47] in the context of classical FEM. In the XFEM framework, a guaranteed procedure for local error estimation was introduced and analyzed in [33]. Based on CRE, the technical point of this procedure is again the construction of admissible fields from the XFEM formulation, and it is easy to show that this construction can be carried out by generalizing the classical procedure detailed in the Appendix.

We choose as quantities of interest the stress intensity factors K_I and K_{II}, and use asymptotic extraction functions proposed in [48] and defined over a crown ω surrounding the crack tip:

$$K_\alpha = \int_\omega \varepsilon(\mathbf{u}) : \big(\mathbf{K}\varepsilon(\phi\mathbf{v}_\alpha) - \phi\sigma_\alpha\big)\mathrm{d}\omega - \int_\omega \mathbf{u}\cdot(\sigma_\alpha\nabla\phi)\mathrm{d}\omega \qquad \alpha = I, II \tag{53}$$

In (53), $\mathbf{v}_\alpha$ and σ_α are singular solutions of the reference problem whereas ϕ is a continuous function, defined in the crown ω, that vanishes along the internal boundary $\mathscr{C}_1$ and is 1 along the external boundary $\mathscr{C}_2$. In the following, we consider a circular crown and we use a linear function ϕ defined in polar coordinates as:

$$\begin{cases} \phi(r,\theta) = \frac{R_2 - r}{R_2 - R_1} & \text{for } R_1 \le r \le R_2 \\ \qquad\quad = 0 & \text{otherwise} \end{cases} \tag{54}$$

R_1 and R_2 are radii of circles $\mathscr{C}_1$ and $\mathscr{C}_2$, respectively (Fig. 7).

The error estimate (9) remains valid provided admissible solutions $(\hat{\mathbf{u}}_h, \hat{\sigma}_h)$ and $(\hat{\tilde{\mathbf{u}}}_h, \hat{\tilde{\sigma}}_h)$ are constructed from XFEM approximate solutions. On the one hand, the admissible kinematic field $\hat{\mathbf{u}}_h$ (resp. $\hat{\tilde{\mathbf{u}}}_h$) is chosen equal to the approximate displacement $\mathbf{u}_h$ (resp. $\tilde{\mathbf{u}}_h$). On the other hand, the construction of $\hat{\sigma}_h$ (or $\hat{\tilde{\sigma}}_h$) is performed dividing the structure Ω into two complementary zones Ω_1 and Ω_2 in order to take the two kinds of enrichment used in XFEM into account separately. A similar approach was investigated in [32] with a mesh conforming to the crack.

Zone Ω_2, that surrounds the crack tip, contains the set of nodes which are enriched with functions $F_j(\mathbf{x})$. In this zone, $\hat{\sigma}_h$ is built from Airy functions, i.e. expressing components of $\hat{\sigma}_h$ in the polar basis as:

$$\begin{cases} \hat{\sigma}_{h,rr} = \frac{1}{r^2}\phi_{,\theta\theta} + \frac{1}{r}\phi_{,r} \\ \hat{\sigma}_{h,\theta\theta} = \phi_{,rr} \\ \hat{\sigma}_{h,r\theta} = -(\frac{1}{r}\phi_{,\theta})_{,r} \end{cases} \quad ; \quad \phi(r,\theta) = \sum_{i=1}^{n} r^{\beta_i+2}\gamma_i(\theta) \tag{55}$$

with $\beta_i = \frac{1}{2}(i-2)$. Functions γ_i $(i = 1,\ldots,n)$, that correspond to asymptotic solutions, read:

$$\gamma_i(\theta) = A_i\sin(\beta_i\theta) + B_i\cos(\beta_i\theta) + C_i\sin((\beta_i+2)\theta) + D_i\cos((\beta_i+2)\theta) \tag{56}$$

and constants A_i, B_i, C_i and D_i verify:

$$\begin{cases} B_i + D_i = 0 \quad \text{and} \quad A_i i + C_i(i+2) = 0 & \text{for } \beta_i = 0, 1, 2, \ldots \\ A_i + C_i = 0 \quad \text{and} \quad B_i(i+1/2) + D_i(i+5/2) = 0 & \text{for } \beta_i = -1/2, 1/2, \ldots \end{cases} \tag{57}$$

Optimal values of constants A_i, B_i, C_i and D_i are then determined by solving a minimization problem over Ω_2:

$$\{A_i, B_i, C_i, D_i\} = argmin_{\{A_i', B_i', C_i', D_i'\}} ||\hat{\sigma}_h(\{A_i', B_i', C_i', D_i'\}) - \sigma_h||_{\mathbf{K}^{-1}|\Omega_2} \quad (58)$$

In practice, we only keep the first order term $\beta = -1/2$ ($i = 1$) so that only 4 constants need to be determined. At the end of this step, in order to ensure the continuity of the stress vector at the interface Γ_{12} between Ω_1 and Ω_2, we solve over Ω_1 a new problem with Neumann boundary conditions $\overline{\mathbf{F}}_d = \hat{\sigma}_{h|\Omega_2}\mathbf{n}$ over Γ_{12}.

In zone Ω_1, the construction of $\hat{\sigma}_h$ is performed by extending to XFEM the classical procedure [4] based on a prolongation condition and using FE properties of σ_h (see Appendix). In particular, we take into account discontinuities introduced with the enrichment by function $H(\mathbf{x})$.

The classical procedure used in FEM, that consists in constructing equilibrated tractions $\hat{\mathbf{F}}_h$ over the boundary ∂E of each FE element E before solving local elementary problems, can be directly extended to the XFEM framework noticing that XFEM merely consists in adding new basis functions $\{N_i(\mathbf{x})\}$. The prolongation condition for enriched elements thus becomes:

$$\int_E (\hat{\sigma}_h - \sigma_h)\nabla N_i \mathrm{d}E = 0 \quad ; \quad \int_E (\hat{\sigma}_h - \sigma_h)\nabla (N_i H)\mathrm{d}E = 0 \quad (59)$$

and leads to two relations:

$$\begin{aligned} \int_{\partial E} \eta_E \hat{\mathbf{F}}_h N_i \mathrm{d}S &= \int_E (\sigma_h \nabla N_i - \mathbf{f}_d N_i)\mathrm{d}E = \mathbf{Q}_E(i) \\ \int_{\partial E} \eta_E \hat{\mathbf{F}}_h N_i H \mathrm{d}S &= \int_E (\sigma_h \nabla (N_i H) - \mathbf{f}_d N_i H)\mathrm{d}E = \mathbf{Q}_E^H(i) \end{aligned} \quad (60)$$

Writing (60) for all elements connected to node i defines a local problem. This is illustrated in Fig. 8 for a 2D mesh where two of the four quadrangle elements connected to node i are cut by the crack; we thus obtain in this case:

$$\begin{cases} \mathbf{b}_{14} - \mathbf{b}_{21} = \mathbf{Q}_{E_1}(i) \\ \mathbf{b}_{21} - \mathbf{b}_{32} = \mathbf{Q}_{E_2}(i) \\ \mathbf{b}_{32} - \mathbf{b}_{43} = \mathbf{Q}_{E_3}(i) \\ \mathbf{b}_{43} - \mathbf{b}_{14} = \mathbf{Q}_{E_4}(i) \end{cases} \quad \text{and} \quad \begin{cases} \mathbf{b}_{14} - \mathbf{b}_{21}^H = \mathbf{Q}_{E_1}^H(i) \\ \mathbf{b}_{21}^H - \mathbf{b}_{32} = \mathbf{Q}_{E_2}^H(i) \end{cases} \quad (61)$$

with unknowns $\mathbf{b}_{kl} = \int_{\Gamma_{kl}} \eta_{E_k} \hat{\mathbf{F}}_h N_i \mathrm{d}S$ and $\mathbf{b}_{kl}^H = \int_{\Gamma_{kl}} \eta_{E_k} \hat{\mathbf{F}}_h N_i H \mathrm{d}S$. Properties of σ_h imply that $\sum_E \mathbf{Q}_E(i) = \sum_E \mathbf{Q}_E^H(i) = \mathbf{0}$ and ensure that local problems of type (61) are well-posed.

After computing projections $\mathbf{b}_{ij}$ and $\mathbf{b}_{ij}^H$, we construct tractions along element edges. In the case of edges cut by the crack (for instance Γ_{12} in Fig. 8), tractions are searched under the form:

$$\hat{\mathbf{F}}_h = \hat{\mathbf{F}}_i N_i + \hat{\mathbf{F}}_j N_j + \hat{\mathbf{F}}_i^H N_i H + \hat{\mathbf{F}}_j^H N_j H \quad (62)$$

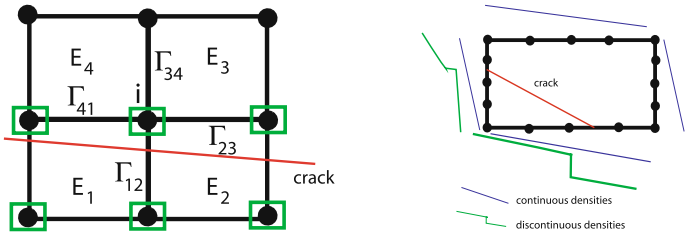

Fig. 8 Patch of elements around node i, with elements E_1 and E_2 cut by the crack, and framed enriched nodes (*left*); local problem to be solved over each element E (*right*)

i.e. as a sum of a continuous part and a discontinuous part. Quantities $\hat{\mathbf{F}}_i, \hat{\mathbf{F}}_j, \hat{\mathbf{F}}_i^H$, and $\hat{\mathbf{F}}_j^H$ can be easily determined by inverting a small linear system implying previously computed projections. Eventually, an admissible stress field $\hat{\sigma}_{h|E}$ is constructed solving a local problem over each element E with Neumann boundary conditions defined by tractions $\hat{\mathbf{F}}_h$. Here again, an enrichment with HN_i functions is used for elements cut by the crack (Fig. 8).

As an illustration, we consider the cracked structure of Fig. 9 clamped on its bottom side and submitted to a uniform shear force density τ on its top side (mixed mode). Parameters are $\tau = 1$, $E = 210$, $\nu = 0.3$, $L = 16$, and $w = 7$. The structure is discretized using a regular mesh with 1071 Q4 elements.

We consider the quantity of interest K_I. We report in Fig. 9 the values of bounds obtained on this quantity of interest. Quantity $K_{I,corr}$ is a correction term, whereas $K_I^{\pm}$ are upper and lower bounds on the exact value of K_I. The reference value, computed using an overkill mesh, is $K_{I,ref} = 33.93$.

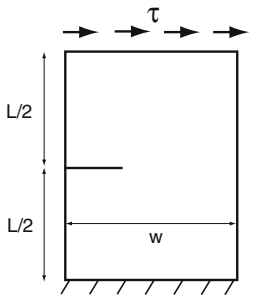

number of elements	$K_{I,h}$	$K_{I,h} + K_{I,corr}$	K_I^-	K_I^+
1071	33.3374	33.6305	32.5714	34.6896
2975	33.3390	33.9100	33.3398	34.4803
5831	33.8579	33.8742	33.5845	34.5845

Fig. 9 Structure with mixed mode loading (*left*), and bounds on K_I for the mixed problem solved with XFEM (*right*)

6.2 PGD-Reduced Models

6.2.1 Context and PGD Strategy

Considering parameterized models (stochastic, optimization), classical approximation methods (mesh grid) lead to an exponential increase in the number of dofs with respect to the number of parameters. This is known as *the curse of dimensionality*, and this rapidly leads to unaffordable computations. Model reduction techniques are alternative tools to address such problems; they have been the object of increasing interest during the previous decade. In particular, an attractive technique called *Proper Generalized Decomposition* (PGD) recently emerged and is currently the topic of various research works [49]. The technique, which leans on ideas initially developed in [50] to solve nonlinear time-dependent problems, is based on variable separation in a spectral approach. The main assets are that no information on the solution is required (contrary to POD) and that the computational cost increases linearly with respect to the number of parameters. PGD basis functions (or modes) are computed on the fly, once for all and in an *offline* process, solving a set of mono-parameter problems with classical techniques. The obtained PGD approximation, that explicitly depends of all model parameters, can then be used in an *online* process for analysis or optimization.

Performances of PGD have been shown in many applications exhibiting changes in loading, boundary or initial conditions, material parameters, geometry, …taken into account by means of additional coordinates in the model [49]. However, a main difficulty for the transfer and intensive use of PGD reduced models in industry is the control of their reliability. Indeed, certifying the PGD solution is fundamental to perform robust design. The control of the PGD solution requires to master the number of modes which are computed (truncation), but also the numerical methods which are employed in the computation of modes.

There are currently very few works addressing the control of PGD approximations. Basic results on a priori error estimation for separated variable representations are given in [50], whereas a pioneering work dedicated to adaptivity can be found in [51]. A first robust approach for the verification of PGD, using the CRE concept, was proposed in [30]. It applies to linear elliptic or parabolic problems depending on parameters, and provides for certified PGD reduced models with respect to global error or error on outputs of interest. Furthermore, the approach enables to assess contributions of the various error sources (space/time discretizations, PGD truncation), which constitutes relevant information to effectively improve the accuracy of the PGD solution. Performances were shown in [30, 52–54] on several numerical experiments implying a transient thermal model with fluctuating material parameters; we provide in the following basic ideas on the approach.

We consider a transient thermal problem defined on domain $\Omega \subset R^d$ $(d = 1, 2, 3)$, with boundary $\partial\Omega$, over the time interval $\mathscr{I} = [0, T]$. A zero temperature is prescribed on boundary $\partial_1\Omega \neq \emptyset$ of $\partial\Omega$ and the time-dependent thermal loading consists of: (i) a given thermal flux $r_d(\mathbf{x}, t)$ on the complementary boundary

$\partial_2\Omega \subset \partial\Omega$; (ii) a source term $f_d(\mathbf{x}, t)$ in Ω. Initial boundary conditions are homogeneous. The material that composes Ω is supposed to be heterogeneous and partially unknown. Therefore, the diffusion tensor $\mathbf{K}$ and the thermal capacity c depend on space variable $\mathbf{x}$ but also on a set of N parameters $\mathbf{p} = [p_1, p_2, \ldots, p_N]$ belonging to a given bounded domain $\Theta = \Theta_1 \times \Theta_2 \times \cdots \times \Theta_N$.

We denote by $(u, \boldsymbol{\varphi})$ the temperature/flux solution of the problem. Defining $\mathscr{U}_{ad} = H_0^1(\Omega) = \{v \in H^1(\Omega), v_{|\partial_1\Omega} = 0\}$, the weak formulation in space of the problem reads for all $(t, \mathbf{p}) \in \mathscr{I} \times \Theta$:

$$\text{Find } u(\mathbf{x}, t, \mathbf{p}) \in \mathscr{U}_{ad} \text{ such that } b(u, v) = l(v) \quad \forall v \in \mathscr{U}_{ad} \tag{63}$$

with $u_{|t=0^+} = 0$. The bilinear form $b(\bullet, \bullet)$ and linear form $l(\bullet)$ are defined as:

$$b(u, v) = \int_\Omega \left\{ c\frac{\partial u}{\partial t} v + \mathbf{K}\nabla u \cdot \nabla v \right\} \mathrm{d}\Omega \quad ; \quad l(v) = \int_\Omega f_d v \mathrm{d}\Omega - \int_{\partial_2\Omega} r_d v \mathrm{d}S \tag{64}$$

We now introduce functional spaces $\mathscr{T} = L^2(\mathscr{I})$, $\mathscr{P}_i = L^2(\Theta_i)$, and $L^2(\mathscr{I}, \Theta; \mathscr{U}_{ad}) = \mathscr{U}_{ad} \otimes \mathscr{T} \otimes_{n=1}^N \mathscr{P}_n$. The full weak formulation of the problem consists in searching $u \in L^2(\mathscr{I}, \Theta; \mathscr{U}_{ad})$, with $\dfrac{\partial u}{\partial t} \in L^2(\mathscr{I}, \Theta; L^2(\Omega))$, such that:

$$B(u, v) = L(v) \quad \forall v \in L^2(\mathscr{I}, \Theta; \mathscr{U}_{ad}) \tag{65}$$

with

$$B(u, v) = \int_\Theta \left[\int_\mathscr{I} b(u, v) \mathrm{d}t + \int_\Omega c u(\mathbf{x}, 0^+) v(\mathbf{x}, 0^+) \mathrm{d}\Omega \right] \mathrm{d}\mathbf{p} \quad ; \quad L(v) = \int_\Theta \int_\mathscr{I} l(v) \mathrm{d}t \mathrm{d}\mathbf{p} \tag{66}$$

The approximate solution of (65), from the FEM in space associated to a given time integration scheme and a given grid in the parameter space Θ, can be very costly when the number of parameters increases.

The alternative PGD technique consists in constructing a priori a separated variable representation of the solution u of (65). The approximate PGD solution is searched under the form:

$$u(\mathbf{x}, t, \mathbf{p}) \approx u_m(\mathbf{x}, t, \mathbf{p}) \equiv \sum_{i=1}^m \psi_i(\mathbf{x}) \lambda_i(t) \Gamma_i(\mathbf{p}) \quad \text{with } \Gamma_i(\mathbf{p}) = \prod_{n=1}^N \gamma_{i,n}(p_n) \tag{67}$$

m is the order (i.e. the number of modes) of the representation, while space functions $\psi_i(\mathbf{x})$, time functions $\lambda_i(t)$, and parameter functions $\gamma_{i,n}(p_n)$ respectively belong to $\mathscr{U}_{ad}$, $\mathscr{T}$ and $\mathscr{P}_n$.

The construction of modes does not require any particular knowledge on u, it is performed on the fly when solving. We give here a classical version of this construction, called *progressive Galerkin* and inspired from classical fixed point algorithms.

We suppose an order $s-1$ PGD approximation has been computed. The order s PGD approximation is then defined as:

$$u_s(\mathbf{x}, t, \mathbf{p}) = u_{s-1}(\mathbf{x}, t, \mathbf{p}) + \psi(\mathbf{x})\lambda(t)\Gamma(\mathbf{p}) \quad \text{with } \Gamma(\mathbf{p}) = \prod_{n=1}^{N} \gamma_n(p_n) \tag{68}$$

ψ, λ, and γ_n ($n = 1, \ldots, N$]) are a priori unknown functions respectively belonging to discretized subspaces $\mathscr{U}_{ad,h}$, $\mathscr{T}_h$, and $\mathscr{P}_{nh}$; we assume that $\mathscr{U}_{ad,h}$ and $\mathscr{T}_h$ verify kinematic constraints and initial conditions, respectively. Starting from initialization $\psi^{(0)}(\mathbf{x})\lambda^{(0)}(t)\Gamma^{(0)}(\mathbf{p})$ for mode s, we construct a new modal representation $\psi^{(1)}(\mathbf{x})\lambda^{(1)}(t)\Gamma^{(1)}(\mathbf{p})$ by means of a Galerkin approach that leads to the following sub-iteration:

$\rightarrow$ find $\lambda^{(1)} \in \mathscr{T}_h$ such that:

$$B(u_{s-1} + \psi^{(0)}\lambda^{(1)}\Gamma^{(0)}, \psi^{(0)}\lambda^*\Gamma^{(0)}) = L(\psi^{(0)}\lambda^*\Gamma^{(0)}) \quad \forall \lambda^* \in \mathscr{T}_h \tag{69}$$

$\rightarrow$ for $n_0 = 1, \ldots, N$, find $\gamma_{n_0}^{(1)} \in \mathscr{P}_{n_0 h}$ such that:

$$B(u_{s-1} + \psi^{(0)}\lambda^{(1)}\gamma_{n_0}^{(1)}\Gamma_{/n_0}^{(1,0)}, \psi^{(0)}\lambda^{(1)}\gamma^*\Gamma_{/n_0}^{(1,0)}) = L(\psi^{(0)}\lambda^{(1)}\gamma^*\Gamma_{/n_0}^{(1,0)}) \quad \forall \gamma^* \in \mathscr{P}_{n_0 h} \tag{70}$$

$$\text{with } \Gamma_{/n_0}^{(1,0)} = \prod_{n=1}^{n_0-1} \gamma_n^{(1)} \times \prod_{n=n_0+1}^{N} \gamma_n^{(0)};$$

$\rightarrow$ find $\psi^{(1)} \in \mathscr{U}_{ad,h}$ such that:

$$B(u_{s-1} + \psi^{(1)}\lambda^{(1)}\Gamma^{(1)}, \psi^*\lambda^{(1)}\Gamma^{(1)}) = L(\psi^*\lambda^{(1)}\Gamma^{(1)}) \quad \forall \psi^* \in \mathscr{U}_{ad,h} \tag{71}$$

The sub-iteration consists in solving a set of simple problems: the ODE in time coming from (69) is solved with an explicit Euler scheme (time step Δt), the space problem coming from (71) is solved with the FEM (mesh size h), while the solution to problems coming from (70) is explicit.

A few sub-iterations are performed in practice. Moreover, the time function $\lambda^{(j)}(t)$ and parameter functions $\gamma_n^{(j)}(p_n)$ are normalized at each sub-iteration. Let us note that a sub-iteration terminates with space problem (71), which is fundamental for the error estimation technique shown in the following. Optimizations, such as updating of the set $\{\lambda_i\}$ (resp. $\{\Gamma_i\}$) of time functions (resp. parameter functions) or orthogonalization of space modes, are possible.

6.2.2 Construction of Equilibrated Fields and Error Estimation

The proposed verification strategy uses the CRE concept. Let $(\hat{u}, \hat{\boldsymbol{\varphi}})$ be an admissible solution to the problem i.e. verifying (in addition to initial conditions) kinematic constraints and balance equations for all $(t, \mathbf{p}) \in \mathscr{I} \times \Theta$. The CRE measure in the space-time domain, that depends on $\mathbf{p}$, thus reads:

$$E^2_{CRE}(\mathbf{p}) = \frac{1}{2}\int_{\mathscr{I}}\int_{\Omega} \mathbf{K}^{-1}[\hat{\boldsymbol{\varphi}} - \mathbf{K}\nabla\hat{u}]\cdot[\hat{\boldsymbol{\varphi}} - \mathbf{K}\nabla\hat{u}]\mathrm{d}\Omega\mathrm{d}t \equiv \frac{1}{2}|||\hat{\boldsymbol{\varphi}} - \mathbf{K}\nabla\hat{u}|||^2_{\mathbf{K}^{-1}} \tag{72}$$

with $|||\bullet|||_{\mathbf{K}^{-1}}$ the energy norm in the space-time domain, and the extension of the Prager-Synge theorem reads:

$$|||\boldsymbol{\varphi} - \hat{\boldsymbol{\varphi}}_m|||^2_{\mathbf{K}^{-1}} + \frac{1}{2}\int_{\Omega} c(u-\hat{u})^2_{|T}\mathrm{d}\Omega = \frac{1}{2}E^2_{CRE} \quad ; \quad \hat{\boldsymbol{\varphi}}_m = \frac{1}{2}[\hat{\boldsymbol{\varphi}} + \mathbf{K}\nabla\hat{u}] \tag{73}$$

Again, the technical point is the construction of an admissible solution; we explain here how such as solution, denoted $(\hat{u}_m, \hat{\boldsymbol{\varphi}}_m)$, can be obtained with a post-processing of all available information from the computation of the PGD solution u_m.

Constructing an admissible kinematic field $\hat{u}_m(\mathbf{x}, t, \mathbf{p})$ is simple, and we choose it equal to $u_m(\mathbf{x}, t, \mathbf{p})$. Obtaining $\hat{\boldsymbol{\varphi}}_m(\mathbf{x}, t, \mathbf{p})$ is more technical; in order to use classical tools that enable to compute equilibrated tractions (in particular the prolongation condition), we should first build a field $\boldsymbol{\varphi}_m(\mathbf{x}, t, \mathbf{p})$ that satisfies the FE equilibrium for all $(t, \mathbf{p}) \in \mathscr{I} \times \Theta$:

$$\int_{\Omega} \boldsymbol{\varphi}_m \cdot \nabla v \mathrm{d}\Omega = \int_{\Omega} (f_d - c\frac{\partial \hat{u}_m}{\partial t})v\mathrm{d}\Omega - \int_{\partial_2\Omega} r_d v \mathrm{d}S \quad \forall v \in \mathscr{U}_{ad,h} \tag{74}$$

We first assume that the external loading can be written under the radial form:

$$(f_d(\mathbf{x}, t), r_d(\mathbf{x}, t)) = \sum_{j=1}^{J} \alpha_j(t)\left(f^j_d(\mathbf{x}), r^j_d(\mathbf{x})\right) \tag{75}$$

We then compute, for each couple (f^j_d, r^j_d), a field $\boldsymbol{\varphi}^j_d(\mathbf{x})$ verifying the FE equilibrium:

$$\int_{\Omega} \boldsymbol{\varphi}^j_d \cdot \nabla v \mathrm{d}\Omega = \int_{\Omega} f^j_d v\mathrm{d}\Omega - \int_{\partial_2\Omega} r^j_d v\mathrm{d}S \quad \forall v \in \mathscr{U}_{ad,h} \tag{76}$$

This computation is in practice performed with the FEM in displacement. This yields, introducing $\boldsymbol{\varphi}_d = \sum_{j=1}^{J} \alpha_j(t)\boldsymbol{\varphi}^j_d(\mathbf{x})$ in (74), that $\boldsymbol{\varphi}_m$ should verify for all $(t, \mathbf{p}) \in \mathscr{I} \times \Theta$:

$$\int_{\Omega} (\boldsymbol{\varphi}_m - \boldsymbol{\varphi}_d)\cdot\nabla v\mathrm{d}\Omega = -\int_{\Omega} c\frac{\partial \hat{u}_m}{\partial t} v\mathrm{d}\Omega = -\sum_{i=1}^{m} c\dot{\lambda}_i\Gamma_i \int_{\Omega} \psi_i v\mathrm{d}\Omega \quad \forall v \in \mathscr{U}_{ad,h} \tag{77}$$

On the other hand, at the end of sub-iterations to compute each PGD mode $m_0 \in [1, m]$, the condition (71) gives:

$$B(u_{m_0}, \psi^*\lambda_{m_0}\Gamma_{m_0}) = L(\psi^*\lambda_{m_0}\Gamma_{m_0}) \quad \forall \psi^* \in \mathscr{U}_{ad,h} \tag{78}$$

This last relation can be recast under the form:

$$\int_\Omega \mathbf{H}_{m_0} \cdot \nabla \psi^* \mathrm{d}\Omega = \int_\Omega \sum_{i=1}^{m_0} \left[G_{m_0,i} \psi_i \right] \psi^* \mathrm{d}\Omega \quad \forall \psi^* \in \mathscr{U}_{ad,h} \tag{79}$$

with

$$\mathbf{H}_{m_0} \equiv \int_\Theta \int_{\mathscr{I}} \lambda_{m_0} \Gamma_{m_0} (\boldsymbol{\varphi}_d - \mathbf{K} \nabla u_{m_0}) \mathrm{d}t \mathrm{d}\mathbf{p} \quad ; \quad G_{m_0,i} \equiv \int_\Theta \int_{\mathscr{I}} c \lambda_{m_0} \Gamma_{m_0} \dot{\lambda}_i \Gamma_i \mathrm{d}t \mathrm{d}\mathbf{p} \tag{80}$$

Consequently, for all $m_0 \in [1, m]$, the term $\mathbf{H}_{m_0}$ equilibrates $\sum_{i=1}^{m_0} G_{m_0,i} \psi_i$ in the FE sense. A simple inversion thus generates terms of the form $\sum_{j=1}^{m} R_{ij} \mathbf{H}_j$ that equilibrate each function ψ_i $(i = 1, \ldots, m)$ in the FE sense. A field $\boldsymbol{\varphi}_m$ that satisfies the FE equilibrium (74) (or (77)) thus reads:

$$\boldsymbol{\varphi}_m = \boldsymbol{\varphi}_d - \sum_{i=1}^{m} \sum_{j=1}^{m} c \dot{\lambda}_i \Gamma_i R_{ij} \mathbf{H}_j \tag{81}$$

From $\boldsymbol{\varphi}_m$, usual techniques can then be used to compute a flux $\hat{\boldsymbol{\varphi}}_m$ that verifies strict equilibrium:

$$\int_\Omega \hat{\boldsymbol{\varphi}}_m \cdot \nabla v \mathrm{d}\Omega = \int_\Omega (f_d - c \frac{\partial \hat{u}_m}{\partial t}) v \mathrm{d}\Omega - \int_{\partial_2 \Omega} r_d v \mathrm{d}S \quad \forall v \in \mathscr{U}_{ad} \tag{82}$$

This flux reads $\hat{\boldsymbol{\varphi}}_m = \hat{\boldsymbol{\varphi}}_d - \sum_{i=1}^{m} \sum_{j=1}^{m} c \dot{\lambda}_i \Gamma_i R_{ij} \hat{\mathbf{H}}_j$ where $\hat{\boldsymbol{\varphi}}_d$ and $\hat{\mathbf{H}}_j$ are computed solving local problems on each element.

Remark 8 In the case of a stationary problem, terms $\mathbf{H}_{m_0} = \int_\Theta \Gamma_{m_0} (\boldsymbol{\varphi}_d - \mathbf{K} \nabla u_{m_0}) \mathrm{d}\mathbf{p}$ $(m_0 = 1, \ldots, m)$ are self-equilibrated in the FE sense. Therefore, $\boldsymbol{\varphi}_m$ and $\hat{\boldsymbol{\varphi}}_m$ can be defined as:

$$\boldsymbol{\varphi}_m(\mathbf{x}, \mathbf{p}) = \boldsymbol{\varphi}_d(\mathbf{x}) + \sum_{m_0=1}^{m} \beta_{m_0}(\mathbf{p}) \mathbf{H}_{m_0}(\mathbf{x}) \quad ; \quad \hat{\boldsymbol{\varphi}}_m(\mathbf{x}, \mathbf{p}) = \hat{\boldsymbol{\varphi}}_d(\mathbf{x}) + \sum_{m_0=1}^{m} \beta_{m_0}(\mathbf{p}) \hat{\mathbf{H}}_{m_0}(\mathbf{x}) \tag{83}$$

where coefficients β_{m_0}, functions of $\mathbf{p}$, are explicitly obtained minimizing $\int_\Theta E^2_{CRE}(\mathbf{p}) \mathrm{d}\mathbf{p}$.

From the global error estimate $E^2_{CRE}(\mathbf{p})$ previously defined, it is then easy to construct a local error estimate from adjoint-based techniques. Let $Q(\mathbf{p})$ be a quantity of interest defined by extractors $(\tilde{\boldsymbol{\varphi}}_\Sigma, \tilde{f}_\Sigma)$:

$$Q(\mathbf{p}) = \int_{\mathscr{I}} \int_\Omega \left(\nabla u(\mathbf{p}) \cdot \tilde{\boldsymbol{\varphi}}_\Sigma + u(\mathbf{p}) \tilde{f}_\Sigma \right) \mathrm{d}\Omega \mathrm{d}t \tag{84}$$

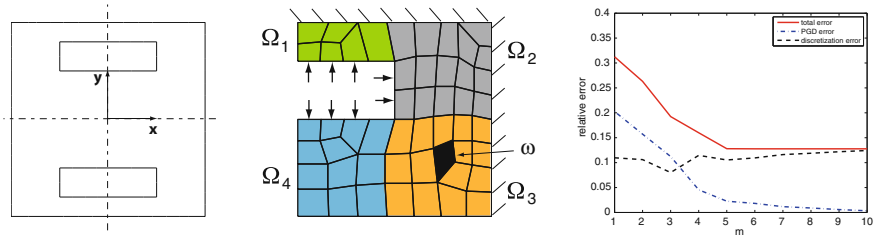

Fig. 10 Representation of the multi-parameter 2D problem (*left*), and relative local error estimate and indicators on the various error sources with respect to the number m of PGD modes for Q_Θ (*right*)

We introduce the associated adjoint problem, and we compute an approximate (resp. admissible) PGD solution $(\tilde{u}_{\widetilde{m}}, \tilde{\boldsymbol{\varphi}}_{\widetilde{m}})$ (resp. $(\hat{\tilde{u}}_{\widetilde{m}}, \hat{\tilde{\boldsymbol{\varphi}}}_{\widetilde{m}})$) for this problem. In practice, the PGD solution to the adjoint problem is performed with an order $\widetilde{m}$ potentially different from m, and introducing enrichment functions locally. We obtain the bounding:

$$|Q(\mathbf{p}) - Q_m(\mathbf{p}) - Q_{corr}(\mathbf{p})| \leq E_{CRE}(\mathbf{p}).\tilde{E}_{CRE}(\mathbf{p}) \tag{85}$$

where $Q_{corr}(\mathbf{p})$ is a computable correction term, and $E_{CRE}(\mathbf{p})$ (resp. $\tilde{E}_{CRE}(\mathbf{p})$) is the constitutive relation error for the reference problem (resp. adjoint problem). Therefore, guaranteed bounds on the local error $Q(\mathbf{p}) - Q_m(\mathbf{p})$ (or directly on $Q(\mathbf{p})$) can be obtained for any value $\mathbf{p}$ of the model parameters.

As an example, we consider the 2D structure represented on Fig. 10. It is a cross section Ω with two rectangular holes in which a fluid circulates. Using symmetries, only a quarter of the structure is considered. A flux $r_d(t) = -1$ is applied on hole boundaries whereas a source term $f_d(x, y) = 200xy$ is applied in Ω. A zero temperature is imposed on the remainder of $\partial\Omega$. We consider that the diffusion coefficient $\mathbf{K}$ (isotropic behavior) fluctuates but remains piecewise homogeneous, i.e. homogeneous in each of the four subdomains Ω_i $(i = 1, 2, 3, 4)$ defined on Fig. 10 and such that $\Omega_i \cap \Omega_j = \emptyset$, $\overline{\Omega_1 \cup \Omega_2 \cup \Omega_3 \cup \Omega_4} = \Omega$. The thermal capacity c is assumed to be homogeneous in the whole domain Ω. These two material coefficients are thus defined by 5 parameters $(\theta_1, \theta_2, \theta_3, \theta_4, \theta_5)$ such that:

$$K(\mathbf{x}, \theta_i) = 1 + \sum_{i=1}^{4} g_i I_{\Omega_i}(\mathbf{x})\theta_i \qquad c(\mathbf{x}, \theta_5) = 1 + 0.2\,\theta_5 \tag{86}$$

with $[g_1, g_2, g_3, g_4] = [0.1; 0.1; 0.2; 0.05]$, and $I_{\Omega_i}(\mathbf{x})$ referring to the indicatrix function of subdomain Ω_i.

The resulting solution $u(\mathbf{x}, t, \mathbf{p})$, with $\mathbf{p} = [\theta_1, \theta_2, \theta_3, \theta_4, \theta_5]$, is searched using the PGD technique; with an initial discretization made of 50 Q4 elements in space and 1000 time steps.

We consider that parameters θ_i are reduced centered (truncated) stochastic variables, with $\theta_i \in [-2, 2]$ ($i = 1, \ldots, 5$). We choose as the quantity of interest the mathematical expectation of the mean temperature in the local zone $\omega \subset \Omega$ (Fig. 10) at final time T:

$$Q(\mathbf{p}) = \frac{1}{|\omega|} \int_{\omega} u(\mathbf{p})_{|T} \mathrm{d}\Omega \quad ; \quad Q_\Theta = \mathrm{E}_\Theta \left[Q(\mathbf{p}) \right] \tag{87}$$

The relative local error $\int_\Theta E_{CRE}.\tilde{E}_{CRE}\mathrm{d}\mathbf{p}/(Q_{\Theta,m} + Q_{\Theta,corr})$ associated to Q_Θ, as well as relative indicators on discretization and truncation errors, are given in Fig. 10 with respect to m.

6.2.3 Adaptive Strategy

The error on Q comes from two sources: (i) the order m truncation of the PGD representation (67); (ii) the space-time discretization used to compute modes numerically. We can write:

$$Q - Q_m = [Q(u) - Q(u^{h,\Delta t})] + [Q(u^{h,\Delta t}) - Q(u_m)] = \Delta Q_{dis} + \Delta Q_{trunc} \tag{88}$$

with ΔQ_{trunc} (resp. ΔQ_{dis}) the part on the error on Q coming from the PGD truncation (resp. from the discretization). $u^{h,\Delta t}$ is the solution to the problem arising from the discretization of (65) and seen as the reference problem to define the error ΔQ_{trunc}.

To effectively control the process of PGD computation, we introduce an error indicator for each error source. The evaluation of ΔQ_{trunc} is performed from CRE taking as the reference problem the discretized problem (with solution $u^{h,\Delta t}$) which can be put under the form:

$$\mathbf{U}_h^1 = \mathbf{0} \quad ; \quad \mathbb{M}(\mathbf{p}) \frac{\mathbf{U}_h^{k+1} - \mathbf{U}_h^k}{\Delta t} + \mathbb{K}(\mathbf{p}) \mathbf{U}_h^k = \mathbf{F}_h^k \quad \forall k \geq 1 \tag{89}$$

with $\mathbf{U}_h^k$ the vector of nodal unknowns of u at time point k. An admissible solution is reconstructed in the sense of the discretized problem by direct post-processing of available information. The evaluation of ΔQ_{dis} is then obtained by the difference between those of $Q - Q_m$ and of ΔQ_{trunc}.

From then on, a simple adaptive strategy consists in evaluating, after the computation of each PGD mode, the various error sources on Q and to adapt with respect to the dominating source: if $|\Delta Q_{dis}|$ is dominating, we define a finer discretization (up to obtaining $|\Delta Q_{dis}| < |\Delta Q_{trunc}|$); if $|\Delta Q_{trunc}|$ is dominating, we compute the next PGD mode without modifying the discretization parameters.

For the same test case, we perform the adaptive procedure (greedy algorithm) coming from the evaluation of error sources. The convergence of the relative local error obtained for Q_Θ is shown in Fig. 11. Vertical evolutions of the curves indicate

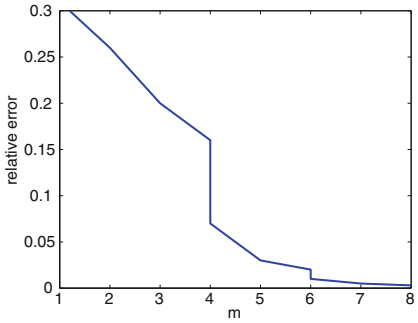

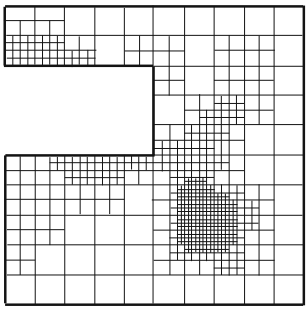

Fig. 11 Convergence of the relative error with respect to the number m of PGD modes in the adaptive strategy for Q_Θ (*left*), and refined mesh used for the computation of PGD mode $m = 8$ after applying the adaptive strategy (*right*)

mesh refinement. We observe that the procedure enables to effectively decrease the error on Q_Θ. Up to mode 4, the initial coarse discretization is sufficient to compute the PGD solution, and the local error decreases when computing a new mode. After $m = 4$, PGD modes represent finer details that require the modification of the discretization parameters. This is illustrated in Fig. 11 where we represent the refined mesh (*quad-tree* structure) used for the computation of the eighth PGD mode, for the adaptive strategy related to Q_Θ.

7 Conclusions and Prospects

We have presented the main aspects and capabilities of error estimation techniques based on the CRE concept. These robust techniques provide for bounds which are both guaranteed and accurate for a large class of mechanical problems, as well as relevant information to drive adaptive processes. Several remaining research issues will be addressed in the near future, such as accurate bounds for complex nonlinear material behavior (with possible softening, instabilities, or large deformations).

Appendix: Construction of Equilibrated Stress Fields

The construction of a statically admissible field is a key point of error estimation methods based on CRE. It particularly enables to obtain guaranteed error bounds for a large set of mechanical problems. A general construction approach, based on a post-processing of the FE stress field σ_h, has been introduced in [4, 35]. This approach, recently named EET (Element Equilibration Technique), can be decomposed in two steps:

1. tractions $\hat{\mathbf{F}}_h$, equilibrated with the external loading, are built on element edges;
2. in each element E, a stress field $\hat{\sigma}_{h|E}$ that verifies equilibrium:

$$\mathbf{div}\,\hat{\sigma}_h + \mathbf{f}_d = \mathbf{0} \text{ in } E \quad ; \quad \hat{\sigma}_h \mathbf{n} = \eta_E \hat{\mathbf{F}}_h \text{ on } \partial E \tag{90}$$

is computed, with $\eta_E = \pm 1$ a scalar value ensuring the continuity of the stress vector. The associated local problem is in practice solved with a quasi-explicit technique and polynomial basis, or with a dual approach with p enrichment (shape functions of degree $p + k$).

The first step leans on the following prolongation (energy) condition:

$$\int_E (\hat{\sigma}_h - \sigma_h)\nabla\phi_i \mathrm{d}E = 0 \quad \Longrightarrow \quad \int_{\partial E} \hat{\sigma}_h \cdot \mathbf{n}\phi_i \mathrm{d}S = \int_E (\sigma_h \nabla\phi_i - \mathbf{f}_d \cdot \phi_i)\mathrm{d}E \quad \forall i \tag{91}$$

where ϕ_i is the FE shape function associated to node i. This condition, which ensures equilibration of $\hat{\mathbf{F}}_h$ over E (as $\sum_i \phi_{i|E} = 1$), leads to the solution to a system of the form:

$$\sum_{r=1}^{R_n} \mathbf{b}_n^r(i) = \mathbf{Q}_{E_n}(i) \quad \forall n = 1, \ldots, N \tag{92}$$

over the set of N elements connected to each node i. R_n is the number of edges for element E_n connected to node i, $\mathbf{Q}_{E_n}(i) = \int_{E_n} (\sigma_h \nabla\phi_i - \mathbf{f}_d\phi_i)\mathrm{d}E$, and unknowns $\mathbf{b}_n^r(i)$ are projections of tractions defined as $\hat{\mathbf{b}}_n^r(i) = \int_{\Gamma_{E_n}^r} \eta_{E_n} \hat{\mathbf{F}}_h \phi_i \mathrm{d}S$. Existence of a solution for each system is ensured by the equilibrium property (in the FE sense) verified by σ_h, and uniqueness may be obtained minimizing a cost function.

In [26], a new hybrid method called EESPT (Element Equilibration + Star Patch Technique) was introduced for the construction of admissible stress fields. As an intermediary between EET and SPET (flux-free [55, 56]) methods, it enables a nice compromise between accuracy of the computed stress fields, computational cost, and practical implementation in engineering softwares. The EESPT method still has two steps and leans on the construction of equilibrated tractions $\hat{\mathbf{F}}_h$ on element edges. The main change is in the way the tractions are constructed, with an increasing flexibility brought by a Partition of Unity Method (PUM); this leads to patch problems solved in an automatic and non-intrusive manner, from classical FE tools. The computation of $\hat{\sigma}_h$, over each element and from tractions $\hat{\mathbf{F}}_h$, remains unchanged and can be parallelized.

A comparison between EET, SPET and EESPT methods was performed in [36] on several industrial applications, one of them being the structure presented in Fig. 2. It was observed that the SPET method is more accurate than EET and EESPT methods, but it requires higher computational cost. The EESPT method, which provides results comparable to those of the EET method, seems to be a nice compromise between accuracy, computational cost and implementation issues.

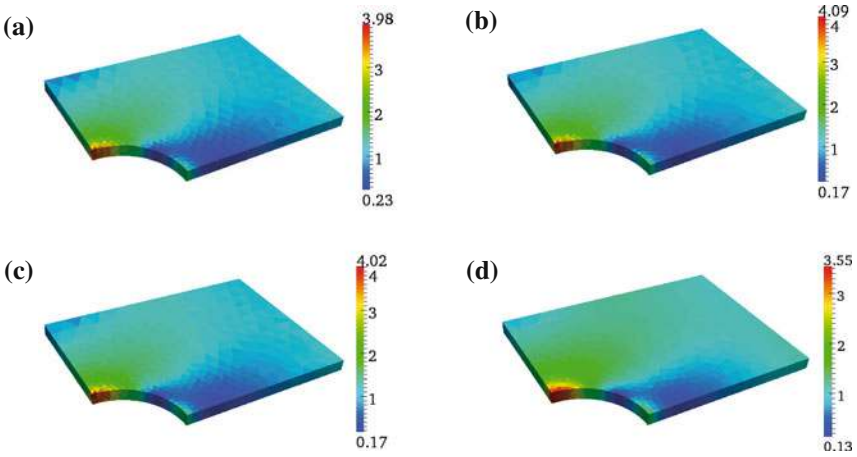

Fig. 12 Norm of the FE stress field (**a**), and admissible stress fields computed with EET (**b**), standard SPET (**c**), and enhanced SPET (**d**) methods

In [57], an improved version of the EESPT method was studied. It uses ideas developed in [58] by considering a weak prolongation condition applied to high degree shape functions (non-vertex nodes). This results in a local minimization of the complementary energy and leads to optimized tractions in selected regions, particularly those with distorted elements or high gradients. The improved version of the EESPT method having a higher computational cost, criteria were introduced to select zones in which this version should be employed to get a nice compromise between accuracy and cost. One example is that of a plate with a hole subjected to a unit traction force (see Fig. 12). EET, standard EESPT, and enhanced EESPT methods were used to compute, from σ_h, a SA stress field $\hat{\sigma}_h$ and derive the associated CRE error estimate. Two criteria were introduced to detect zones in which the enhanced SPET method should be used; the first criterion is based on the element shape (distorsion level) and thus relies on the local quality of the mesh, whereas the second criterion considers local error contributions.

References

1. I. Babuška, T. Strouboulis, *The Finite Element Method and Its Reliability* (Oxford University Press, Oxford, 2001)
2. N.E. Wiberg, P. Diez, Special issue. Comput. Methods Appl. Mech. Eng. **195**, 4–6 (2006)
3. P. Ladevèze, J.-T. Oden, *Advances in Adaptative Computational Methods in Mechanics* (Elsevier, New York, 1998)
4. P. Ladevèze, J.-P. Pelle, *Mastering Calculations in Linear and Nonlinear Mechanics* (Springer, New York, 2004)
5. E. Stein, *Error Controlled Adaptive Finite Elements in Solid Mechanics* (Wiley, Chichester, 2003)

6. P. Ladevèze, Comparison of continuum mechanics models (in French). PhD Thesis, Paris 6 University (1975)
7. I. Babuška, W.C. Rheinboldt, A posteriori error estimates for the finite element method. Int. J. Numer. Meth. Eng. **12**, 1597–1615 (1978)
8. O.C. Zienkiewicz, J.Z. Zhu, A simple error estimator and adaptive procedure for practical engineering analysis. Int. J. Numer. Meth. Eng. **24**, 337–357 (1987)
9. P. Ladevèze, P. Rougeot, P. Blanchard, J.P. Moreau, Local error estimators for finite element linear analysis. Comput. Methods Appl. Mech. Eng. **176**, 231–246 (1999)
10. J. Peraire, A.T. Patera, in *Bounds for Linear-functional Outputs of Coercive Partial Differential Equations: Local Indicators and Adaptive Refinements*, eds. by P. Ladevèze, J.-T. Oden. Advances in Adaptive Computational Methods in Mechanics (Elsevier, New York, 1998), pp. 199–216
11. S. Prudhomme, J.T. Oden, On goal-oriented error estimation for elliptic problems: application to the control of pointwise errors. Comput. Methods Appl. Mech. Eng. **176**, 313–331 (1999)
12. R. Rannacher, F.T. Suttmeier, in *A Posteriori Error Control and Mesh Adaptation for Finite Element Models in Elasticity and Elasto-plasticity*, eds. by P. Ladevèze, J.-T. Oden. Advances in Adaptative Computational Methods in Mechanics (Elsevier, New York, 1998), pp. 275–292
13. T. Strouboulis, I. Babuška, D. Datta, K. Copps, S.K. Gangaraj, A posteriori estimation and adaptive control of the error in the quantity of interest—part 1: a posteriori estimation of the error in the Von Mises stress and the stress intensity factors. Comput. Methods Appl. Mech. Eng. **181**, 261–294 (2000)
14. R. Becker, R. Rannacher, A feed-back approach to error control in finite element methods: basic analysis and examples. East-West J. Numer. Math. **4**, 237–264 (1996)
15. K. Eriksson, D. Estep, P. Hansbo, C. Johnson, in *Introduction to Adaptive Methods For Partial Differential Equations*, ed. by A. Isereles. Acta Numerica (Cambridge University Press, Cambridge, 1995), pp. 105–159
16. F. Cirak, E. Ramm, A posteriori error estimation and adaptivity for linear elasticity using the reciprocal theorem. Comput. Methods Appl. Mech. Eng. **156**, 351–362 (1998)
17. N. Parès, J. Bonet, A. Huerta, J. Peraire, The computation of bounds for linear-functional outputs of weak solutions to the two-dimensional elasticity equations. Comput. Methods Appl. Mech. Eng. **195**(4–6), 406–429 (2006)
18. H.J. Greenberg, The determination of upper and lower bounds for the solution of Dirichlet problem. J. Math. Phys. **27**, 161–182 (1948)
19. K. Washizu, Bounds for solutions of boundary value problems in elasticity. J. Math. Phys. **32**, 117–128 (1953)
20. P. Ladevèze, Upper error bounds on calculated outputs of interest for linear and nonlinear structural problems. Comptes Rendus Acadmie des Sciences—Mcanique, Paris **334**, 399–407 (2006)
21. P. Ladevèze, B. Blaysat, E. Florentin, Strict upper bounds of the error in calculated outputs of interest for plasticity problems. Comput. Methods Appl. Mech. Eng. **245–246**, 194–205 (2012)
22. J. Waeytens, L. Chamoin, P. Ladevèze, Guaranteed error bounds on pointwise quantities of interest for transient viscodynamics problems. Comput. Mech. **49**(3), 291–307 (2012)
23. L. Chamoin, P. Ladevèze, Bounds on history-dependent or independent local quantities in viscoelasticity problems solved by approximate methods. Int. J. Numer. Meth. Eng. **71**(12), 1387–1411 (2007)
24. L. Chamoin, P. Ladevèze, A non-intrusive method for the calculation of strict and efficient bounds of calculated outputs of interest in linear viscoelasticity problems. Comput. Methods Appl. Mech. Eng. **197**(9–12), 994–1014 (2008)
25. P. Ladevèze, L. Chamoin, Calculation of strict error bounds for finite element approximations of nonlinear pointwise quantities of interest. Int. J. Numer. Meth. Eng. **84**, 1638–1664 (2010)
26. P. Ladevèze, L. Chamoin, E. Florentin, A new non-intrusive technique for the construction of admissible stress fields in model verification. Comput. Methods Appl. Mech. Eng. **199**(9–12), 766–777 (2010)

27. P. Ladevèze, F. Pled, L. Chamoin, New bounding techniques for goal-oriented error estimation applied to linear problems. Int. J. Numer. Meth. Eng. **93**, 1345–1380 (2013)
28. L. Chamoin, E. Florentin, S. Pavot, V. Visseq, Robust goal-oriented error estimation based on the constitutive relation error for stochastic problems. Comput. Struct. **106–107**, 189–195 (2012)
29. P. Ladevèze, Strict upper error bounds for computed outputs of interest in computational structural mechanics. Comput. Mech. **42**(2), 271–286 (2008)
30. P. Ladevèze, L. Chamoin, On the verification of model reduction methods based on the Proper Generalized Decomposition. Comput. Methods Appl. Mech. Eng. **200**, 2032–2047 (2011)
31. P. Ladevèze, J. Waeytens, Model verification in dynamics through strict upper error bounds. Comput. Methods Appl. Mech. Eng. **198**(21–26), 1775–1784 (2009)
32. J. Panetier, P. Ladevèze, F. Louf, Strict bounds for computed stress intensity factors. Comput. Struct. **871**(15–16), 1015–1021 (2009)
33. J. Panetier, P. Ladevèze, L. Chamoin, Strict and effective bounds in goal-oriented error estimation applied to fracture mechanics problems solved with the XFEM. Int. J. Numer. Meth. Eng. **81**(6), 671–700 (2010)
34. P. Ladevèze, E.A.W. Maunder, A general method for recovering equilibrating element tractions. Comput. Methods Appl. Mech. Eng. **137**, 111–151 (1996)
35. P. Ladevèze, D. Leguillon, Error estimate procedure in the finite element method and application. SIAM J. Numer. Anal. **20**(3), 485–509 (1983)
36. F. Pled, L. Chamoin, P. Ladevèze, On the techniques for constructing admissible stress fields in model verification: performances on engineering examples. Int. J. Numer. Meth. Eng. **88**(5), 409–441 (2011)
37. P. Ladevèze, J.L. Gastine, P. Marin, J.P. Pelle, Accuracy and optimal meshes in finite element computation for nearly incompressible materials. Comput. Methods Appl. Mech. Eng. **94**(3), 303–314 (1992)
38. W. Prager, J.L. Synge, Approximation in elasticity based on the concept of functions spaces. Q. Appl. Math. **5**, 261–269 (1947)
39. P. Ladevèze, N. Moës, A new a posteriori error estimation for nonlinear time-dependent finite element analysis. Comput. Methods Appl. Mech. Eng. **157**, 45–68 (1998)
40. N. Moës, J. Dolbow, T. Belytschko, A finite element method for crack growth without remeshing. Int. J. Numer. Meth. Eng. **46**, 131–150 (1999)
41. T. Strouboulis, I. Babuška, K. Copps, The design and analysis of the generalized finite element method. Comput. Methods Appl. Mech. Eng. **181**(1–3), 43–69 (2000)
42. R.D. Mindlin, Force at a point in the interior of a semi-infinite solid. J. Phys. **7**, 195–202 (1936)
43. S. Vijayakumar, E.C. Cormack, Green's functions for the biharmonic equation: bonded elastic media. SIAM J. Appl. Math. **47**(5) (1987)
44. M. Dahan, M. Predeleanu, Solutions fondamentales pour un milieu élastique à isotropie transverse. ZAMP **31**, 413–424 (1980)
45. P. Ladevèze, E. Florentin, Verification of stochastic models in uncertain environments using the constitutive relation error method. Comput. Methods Appl. Mech. Eng. **196**, 225–234 (2006)
46. L. Gallimard, J. Panetier, Error estimation of stress intensity factors for mixed-mode cracks. Int. J. Numer. Meth. Eng. **68**(3), 299–316 (2006)
47. T.J. Stone, I. Babuška, A numerical method with a posteriori error estimation for determining the path taken by a propagating crack. Comput. Methods Appl. Mech. Eng. **160**, 245–271 (1998)
48. I. Babuška, A. Miller, The post-processing approach in the finite element method—part 2: the calculation of stress intensity factors. Int. J. Numer. Methods Eng. **20**, 1111–1129 (1984)
49. F. Chinesta, A. Ammar, E. Cueto, Recent advances and new challenges in the use of the proper generalized decomposition for solving multidimensional models. Arch. Comput. Methods Eng. **17**(4), 327–350 (2010)
50. P. Ladevèze, *Nonlinear Computational Structural Mechanics—New Approaches and Non-Incremental Methods of Calculation* (Springer, New York, 1999)

51. A. Ammar, F. Chinesta, P. Diez, A. Huerta, An error estimator for separated representations of highly multidimensional models. Comput. Methods Appl. Mech. Eng. **199**, 1872–1880 (2010)
52. P.E. Allier, L. Chamoin, P. Ladevèze, Proper Generalized Decomposition computational methods on a benchmark problem. Submitted to AMSES (2015)
53. L. Chamoin, P. Ladevèze, Robust control of PGD-based numerical simulations. Eur. J. Comput. Mech. **21**(3–6), 195–207 (2012)
54. P. Ladevèze, L. Chamoin, in *Toward Guaranteed PGD-reduced Models*, eds. by G. Zavarise, D.P. Boso. Bytes and Science (CIMNE, 2012)
55. N. Pares, P. Diez, A. Huerta, Subdomain-based flux-free a posteriori error estimators. Comput. Methods Appl. Mech. Eng. **195**(4–6), 297–323 (2006)
56. J.P. Moitinho de Almeida, E.A.W. Maunder, Recovery of equilibrium on star patches using a partition of unity technique. Int. J. Numer. Meth. Eng. **79**, 1493–1516 (2009)
57. F. Pled, L. Chamoin, P. Ladevèze, An enhanced method with local energy minimization for the robust a posteriori construction of equilibrated stress fields in finite element analyses. Comput. Mech. **49**(3), 357–378 (2012)
58. E. Florentin, L. Gallimard, J.P. Pelle, Evaluation of the local quality of stresses in 3D finite element analysis. Comput. Methods Appl. Mech. Eng. **191**, 4441–4457 (2002)